Behaviour of recycled tyre polymer fibre reinforced concrete at elevated temperatures

Meng Chen [a], Zhihao Sun [a], Wenlin Tu [b], Xin Yan [a], Mingzhong Zhang [b,*]

[a] School of Resources and Civil Engineering, Northeastern University, Shenyang, 110819, China

[b] Department of Civil, Environmental and Geomatic Engineering, University College London, London, WC1E 6BT, UK

Abstract: This paper presents a systematic study on the feasibility of using recycled tyre polymer (RTP) fibres for mitigating the damage of concrete induced by elevated temperatures. A series of tests were conducted to investigate the effect of RTP fibres on mechanical and thermal behaviour, pore pressure build-up and microstructural evolution of concrete exposed to elevated temperatures (20, 105, 250, 400 and 600 °C), based on which the mechanism of RTP fibres in mitigating damage of concrete was explored. Results indicate that the addition of RTP fibres effectively prevented pore pressure accumulation and significantly mitigated damage of concrete at high temperatures as the melting of RTP fibres and thermal incompatibility between RTP fibres and concrete promoted the formation of interconnected pore-microcrack network of concrete. RTP fibre was proved as a promising sustainable alternative to manufactured polymer fibres for enhancing high temperature and fire resistance of concrete. The optimal RTP fibre content was 1.2 kg/m^3 considering the damage mitigation efficiency and strength loss.

Keywords: Fibre reinforced concrete; Recycled fibre; Microstructure; Pore pressure; Thermal analysis

1. Introduction

High-temperature issue has always been concerned as one of the most serious risks for large-scale concrete structures [1, 2]. For instance, the Grenfell Tower fire in Kensington, London, was one of the catastrophes that killed 74 people in a 24-storey building in 2017 [3]. When subjected to elevated temperatures, concrete would experience damage or even spalling with development of cracks and loss of concrete cover, leading to direct exposure of steel reinforcement to high-temperature environment and reduction in the load-carrying capacity of reinforced concrete structures [4-7]. The damage mechanisms of concrete at high temperatures have been extensively studied and widely accepted as a combination of two aspects: (1) thermo-hygral: accumulation of internal pore pressure due to difficulties to relieve free water and vapour until it exceeds the threshold value [8]; (2) thermomechanical: thermal stresses that develop along the heated surface [9]. The pore pressure induced damage is highly dependent on microcracks and pore structure of concrete, whereas the thermal stress induced damage takes place near the heated surface in the form of concrete compression failure, which is significantly associated with heating rate [10].

To tackle the potential risks of such damage of concrete subjected to elevated temperatures and enhance thermal and fire resistance of concrete, many efforts have been made over the past decades. The commonly used approaches include the incorporation of steel fibres, polymer fibres and hybrid fibres [11-17]. Steel fibres melt at temperatures higher than 1300 °C [18]. Therefore, adding steel fibres can result in an augment of tensile strength of concrete by retaining fibre bridging effect over a large temperature range, so that fire endurance of concrete can be improved [8, 18]. Steel fibres can also withstand and mitigate pore pressure by entrapping air bubbles around the fibres to accommodate water and vapour [19]. It was reported that concrete with 1% (by volume of binder, V_f) steel fibre improved residual flexural strength by 15% compared to plain concrete, which can be attributed to the pull-out resistance of steel fibres [20]. In contrast to steel fibres, polymer fibres such as polyethylene (PE), polyvinyl alcohol (PVA) and polypropylene (PP) fibres melt at much lower temperatures of around 145-230 °C. Hence, instead of crack-bridging effect, the use of polymer fibres was found to improve pore connectivity and permeability of concrete to resist spalling by leaving behind an interconnected network after melting at elevated temperatures [21]. Among these polymer fibres, PP fibre was broadly proved to be the most beneficial in enhancing pore connectivity of concrete matrix and increasing permeability to prevent spalling [15, 21]. Due to the low melting point of PP fibres (around 160 °C), the empty channels they left after exposure to high temperatures were connected with each other, in which moisture and vapour can transport freely without causing any moisture clog and pore pressure accumulation [5, 22, 23], and consequently the explosive spalling can be prevented. The previous studies indicated that spalling can be effectively eliminated under high temperatures when incorporating 0.6% PP fibres into concrete [14]. The addition of 0.1-0.25% PP fibres in concrete was also found to significantly mitigate the spalling as a result of the melting action of PP fibres which released pore pressure through the interconnected network [24]. For concrete reinforced with hybrid steel and PP fibres, there also exhibited a significant reduction in spalling due to the combination of the fibre bridging effect of steel fibres that impeded the initiation and propagation of cracks and the melting effect of PP fibres leading to additional channels for high moisture pressure relief [25, 26].

However, the production of the aforementioned fibres not only emits a significant amount of carbon dioxide that causes environmental pollution, but also requires a large embodied energy consumption during the manufacturing process, which takes up around 15% of the total building energy [27-30]. Therefore, the research interests are moved to seek for alternative materials that can help reduce energy consumption and improve sustainability of fibre reinforced concrete. Recently, a growing emphasis has been placed on the use of end-of-life materials such as recycled tyre fibres as reinforcement for concrete. It was reported that the amount of polymer fibre extracted from waste tyres through thermomechanical treatments (as a by-product) reaches around 63,000 tonnes annually

in the EU alone [31]. The storage of them is a problem as they are flammable and easily carried away by wind and thus pollute the surrounding environment [31-33]. Hence, it is very urgent and vital to explore the feasibility of using recycled tyre polymer (RTP) fibre that is a 'negative-value' waste as a substitute for manufactured PP fibres for concrete to enhance the performance and sustainability of concrete [32].

In recent years, several attempts have been made to investigate engineering properties and durability of RTP fibre reinforced concrete, mainly focusing on the effects of RTP fibres on static and dynamic mechanical properties [34], fatigue behaviour [27] and durability-related performance such as resistance to freeze-thaw cycles [35]. It was found that the incorporation of RTP fibres can reduce early-age shrinkage of concrete and thus tackle mechanical and durability problems [35]. As a replacement of PP fibres, the addition of RTP fibres in concrete can effectively impede the crack development and improve the resistance of concrete to freeze-thaw cycles due to the stress absorption capacity provided by the rubble particles attached on RTP fibres [32]. Concrete specimens reinforced with 2.4 kg/m^3 (0.2% V_f) of RTP fibres exhibited the highest flexural strength with an increase of 9.6% compared to plain concrete, which can be ascribed to the enhanced resistance to crack propagation across the fracture zone and fibre bridging action [27]. The fatigue performance of concrete was also found to be enhanced by 58.3% when adding 4.8 kg/m^3 (0.4% V_f) RTP fibres. Similar fatigue mechanisms were observed for RTP and PP fibre reinforced concrete that experienced three stages including initiation, propagation and simultaneous formation of micro- and macro-cracks, indicating that RTP fibres could be a promising alternative to PP fibres with a suggested ratio of 1:2 to 1:4, i.e., replacing 0.1% V_f of PP fibres with 0.2-0.4% V_f of RTP fibres [27]. Nevertheless, the behaviour of RTP fibre reinforced concrete at elevated temperatures has been rarely studied. Some preliminary experimental work showed that the addition of RTP fibres at a dosage of 2 kg/m^3 could effectively increase fire resistance and prevent spalling of concrete while the fresh and hardened properties of concrete were not significantly affected by fibre incorporation [31, 36, 37]. Although the feasibility of using RTP fibres for mitigating thermal and fire induced damage in concrete was explored from a macroscopic perspective [38], the effect of RTP fibres on physicochemical properties and microstructural evolution of concrete subjected to elevated temperatures have not been systematically studied. In addition, to the best of authors' knowledge, the mechanism of RTP fibres in reducing damage of concrete at elevated temperatures has not been explored. Thus, for the sake of developing a sustainable high-temperature and fire resistant concrete, it is vital to conduct a comprehensive study to evaluate the use of RTP fibres in concrete at elevated temperatures and understand the relevant mechanism.

The main purpose of this study is to systematically investigate the effect of RTP fibre on behaviour of concrete at elevated temperatures and, for the first time, to provide a comprehensive understanding

of damage evolution in RTP fibre reinforced concrete subjected to elevated temperatures. A series of tests were conducted to measure fresh properties as well as mechanical properties, weight loss and pore pressure of concrete with various RTP fibre dosages including 0, 0.6 (0.05% V_f), 1.2 (0.1% V_f), 2.4 (0.2% V_f) and 4.8 kg/m^3 (0.4% V_f) at elevated temperatures, i.e. 20, 105, 250, 400 and 600 °C. Microstructural characteristics of concrete with various RTP fibre content before and after exposure to elevated temperatures were then explored by means of differential scanning calorimeter (DSC), thermogravimetric analysis (TGA), X-ray diffractometer (XRD), scanning electron microscope (SEM) and mercury intrusion porosimetry (MIP), based on which the mechanisms of RTP fibres in mitigating damage of concrete at elevated temperatures were discussed in detail.

2. Experimental program

2.1 Raw materials

Portland cement (P.I. 42.5R) with a specific gravity of 3.09 conforming to the requirements of Chinese standard GB175 [39] was used in this study, the chemical composition of which is given in Table 1. Natural river sand with a density of 1480 kg/m^3 and crushed granite with a nominal size ranging from 5 to 10 mm were used as fine and coarse aggregates, respectively. Polycarboxylate-based superplasticizer (SP) was added to ensure sufficient consistency for all mixtures.

The RTP fibre used in this study was recycled mainly from truck tyres, which is composed of 52% polyethylene terephthalate (PET), 39% polyamide 66 (PA 66) and 9% polybutylene terephthalate (PBT) [40]. It is worth mentioning that several rubber granules were attached on the received RTP fibres. To eliminate the influence of rubber granules on the test results, a sieving process was undertaken to remove them from RTP fibres [27]. Three sieves with sizes of 0.315, 0.63 and 1.25 mm were placed on a vibration table. RTP fibres were firstly placed in the 1.25 mm sieve with six steel balls (8 mm diameter). These steel balls were used to improve the efficiency of sieving during the vibration process. The fine cleaned RTP fibres then fell into the 0.63 mm sieve and eventually passed through the 0.315 mm sieve. The whole procedure was repeated for six times to obtain pure RTP fibres, more details about which can be found in [27]. Fig. 1 shows the morphology of cleaned RTP fibres. The diameter and tensile strength of RTP fibres were measured using XGD-1 Fibre Diameter Tester and XQ-1A Fibre Tensile Tester according to GB/T 21120–2007 [41]. The thermal behaviour of RTP fibres and their weight loss evolution at elevated temperatures were measured using DSC and TGA, the results of which are shown in Fig. 2. As can be seen, the tested RTP fibres exhibited the first exothermic peak at 256 °C and the second exothermic peak at 413 °C, which represent the melting and vaporisation points of the fibres, respectively. Compared to PP fibres that melt at around 171 °C and vaporise at about 341 °C [42], the appearance of these critical points of RTP fibres is postponed to higher temperatures. The properties of RTP fibres are summarised in Table 2. The TGA curve indicates the weight loss of RTP fibre with elevated temperatures due to the melting and

4

decomposition of RTP fibre. A significant weight loss occurs at the temperature ranging from 316-430 °C, suggesting a quick decomposition of RTP fibre after melting.

2.2 Mix proportions

The mix proportions of RTP fibre reinforced concrete studied are shown in Table 3, where all the mixtures had a constant water-to-binder (w/b) ratio of 0.46. In Table 3, the label 'RTPF' stands for RTP fibres, whilst the numbers '06', '12', '24' and '48' represent the specified RTP fibre content. For instance, '06' and '12' correspond to 0.6 kg/m^3 and 1.2 kg/m^3, respectively. A control mixture without RTP fibre was prepared and denoted as RTPF0. Previous studies reported that the incorporation of RTP fibres up to 5 kg/m^3 had no or negligible influence on the mechanical properties of concrete [27, 32, 34]. The optimal RTP fibre content for concrete was found to be 2.4 kg/m^3 considering setting time, workability, and static and dynamic mechanical properties [40]. However, there has been no study on thermal behaviour of RTP fibre reinforced concrete to date. Thus, five different RTP fibre dosages ranging from 0 to 4.8 kg/m^3 were adopted in this study to investigate the behaviour of RTP fibre reinforced concrete at elevated temperatures.

2.3 Sample preparation

The mixing procedure of all five mixtures consists of three steps. Firstly, cement, fine aggregates and coarse aggregates were dry mixed for 1 min to ensure homogeneous dispersion of dry solid ingredients. Then, the measured water (partially used to prepare wet RTP fibres) and SP were added into the mixture, followed by mixing for another 2 min. Finally, the pre-wetted RTP fibres were gradually added into the mixture to avoid fibre balling and mixed until the RTP fibres were evenly dispersed in the mixture. Subsequently, fresh mixtures were immediately poured into specific moulds (100 mm cube for compressive strength test, 50×100 mm cylinder for ultrasonic pulse velocity test, and 200 mm cube for pore pressure test) and then placed on a vibration table for better consolidation and removal of entrapped air. The specimens were de-moulded after 24 h of casting and then stored in a standard curing room (20 ± 2 °C and 95% relative humidity) for 28 d. The surface of the specimens was dried before heating and testing.

There are two main heating methods for concrete specimens: standard heating rate following the curve of ISO-834 and constant heating rate. The standard heating curve of ISO-834 gives an exponential relationship between growing temperature and heating time [11], which defines the temperature-time curve of concrete under fire circumstance. Fire experiments have been extensively conducted to investigate pore pressure of concrete [43, 44], but it is difficult to eliminate potential safety risks when carrying out a fire test in the laboratory and thus a constant heating rate was applied to simplify the heating process instead [11]. By this mean the specimen was heated up in an electric furnace with a constant heating rate until the target temperature was reached. The most commonly used heating rate ranges from 1 to 10 °C/min, such as 1 °C/min [2, 9], 2 °C/min [45], 4 °C/min [46],

5

and 10 °C/min [14, 18, 47]. A higher heating rate can significantly speed up the pore pressure build-up inside concrete due to a higher induced thermal stress [8]. In this study, the heating rate was set as 10 °C/min to attain the target temperatures of 105, 250, 400 and 600 °C. The furnace was maintained at the target temperatures for 180 min that was the dwell time to ensure a uniform distribution of temperature within the specimen. Afterwards, the furnace was switched off and the specimen was cooled down naturally to room temperature.

2.4 Test methods

2.4.1 Workability

The slump test was undertaken to measure the workability of the specimens as per GB/T50080-2016 [48]. Each fresh RTP fibre reinforced concrete mixture was firstly cast into a specified cone to form three layers and jointed for 25 times at each layer. 30 s after filling the testing mould, the slump value was measured as the vertical difference between the top of the mould and the top surface of the specimen.

2.4.2 Ultrasonic pulse velocity

The 50×100 mm cylinder samples of all mixtures were heated up to the specific temperature in the electric furnace (SRJX-4-13, Shenyang) at a heating rate of 10 °C/min. The holding time was 180 min after reaching the target temperatures, i.e. 105, 250, 400 and 600 °C. The UPV test was conducted using an acoustic parameter tester (HS-YS403B) after the specimens were cooled down to room temperature. The coupling gel was added on the top and bottom surfaces of the sample, and then the transducers were placed firmly on them to measure the velocity.

2.4.3 Compressive strength

The 100 mm cube specimens were prepared following the same procedure as mentioned above. The 28-d compressive strength of RTP fibre reinforced concrete at different temperatures was tested using a universal testing machine with a constant loading rate of 9 kN/s in accordance to GB/T50081-2002 [49].

2.4.4 Weight loss

The weight loss was measured based on the weight difference between the specimens before and after heating (recognised as m_1 and m_2, respectively). The weight loss ratio (R_m) can be calculated as:

$$R_m = \frac{(m_1 - m_2)}{m_1} \tag{1}$$

2.4.5 Pore pressure

The pore pressure measurement was carried out according to the experimental setup demonstrated in Fig. 3. The thermal load was applied on the bottom face of a 100 mm cubic concrete specimen, which was placed inside a heat insulation box (250×250×250 mm). Heating with a rate of 10 °C/min to 600 °C was provided by the electric heating wire located at the bottom of the specimen. Three gauges made of a sintered metal plate were placed inside the specimen at casting and brazed to a steel tube

6

with inner diameter of 2 mm, as shown in Fig. 3. At the free end of the steel tube, a connector linking the gauge to a pressure transducer through a soft tube filled with silicone oil was inserted [50]. A thermocouple was also connected to the metal plate. These gauges were placed at 20, 50 and 100 mm from the heated face, respectively.

2.4.6 Thermal analysis

DSC and TGA were carried out to examine the melting and decomposition behaviour of RTP fibre and concrete. The powder specimens (< 0.074 mm) taken from the crushed RTPF0 and RTPF12 samples at ambient temperature after the compressive strength test were used for DSC and TGA tests with the assistance of NETZSCH STA 490PC. A constant heating rate of 10 °C/min from room temperature to 600 °C was employed. The gas flow used was fixed at 50 ml/min. The heat transformation is reflected on the DSC curve, while the TGA curve denotes the weight loss of specimens as a function of temperature. The derivative thermogravimetry (DTG) curve can be determined from the first derivative of the TGA curve.

2.4.7 X-ray diffractometer

To prepare the samples for XRD analysis, a portion of material was extracted from cores retained from the compressive strength test. Each sample was ground into powder until at least 90% passed through a 45 µm sieve. The phases composition of the samples was detected by an XRD (D8 ADVANCE, Malvern Panalytical, Netherlands). The run conditions included CuKα X-ray radiation and scanning at the intensity of 40 kV- 40 mA with the slit system of RS = 0.1 mm and DS = SS = 0.6°; the 2θ scanning rate of 6°/min. The step size was 0.02° with $2\theta = 90°$. The previous studies concluded that there was no obvious difference between the XRD spectra of specimens with and without polymer fibres [9]. Therefore, herein, ethe specimens of RTPF0 under different temperature treatments were used to conduct the test.

2.4.8 Scanning electron microscope

The microstructural evolution of RTP fibre reinforced concrete specimens after exposure to elevated temperatures was detected using SEM. After the non-destructive (UPV) test, the RTPF48 samples were cut, ground and polished to obtain a surface with multiple RTP fibre cross-sections. Prior to viewing in the SEM, the samples were sputter coated twice with gold-palladium. The microscopic observation was then carried out using Ultra Plus to trace fibre cross-section and microcracks before (20 °C) and after exposure to high temperatures and the observation point was marked to ensure that it was positioned at the centre of the SEM. The working distance for the test was set in the range of 10-17 mm. The acceleration voltage and magnification were 15 kV and 400×, respectively.

2.4.9 Mercury intrusion porosimetry

The pore structure of the specimens was characterised using MIP. To prepare the specimens for MIP test, the testing samples were crushed into pieces and those smaller than 500 mm^3 were selected for

each sample. The test was carried out on an AutoPore IV 9500 MIP capable of generating pressure in the range of 0 to 414 MPa. The pore diameter ranging from 0.001 to 1000 µm was measured and the surface tension of mercury employed here was 0.485 N/m. The contact angle between the mercury and the pore surface was 130° [51].

3. Results

3.1 Workability

Workability is an essential fresh property of concrete, which directly determines the feasibility of engineering application of the designed mixtures. Thus, the effect of RTP fibres on the workability of fresh specimens needs to be studied prior to other tests. Fig. 4 shows the slump values of all mixtures with various RTP fibre content in comparison with experimental data obtained from literature [35, 40]. Overall, the slump value decreases with the increase of RTP content, which is consistent with that presented in [35, 40]. As the RTP dosage increases from 0 to 4.8 kg/m^3, the slump value is reduced from 176 mm to 86 mm. In comparison with that of control mixture (RTPF0), the slump results of specimens with RTP fibres are declined by 5.1% to 51.5% (from RTPF06 to RTPF48). This can be attributed to the shear resistance induced by the addition of RTP fibres, which impedes the flow of fresh mixtures and thereby reduces the slump value [27]. Furthermore, during the mixing process, a certain amount of water may be absorbed by RTP fibres to moist the rubber granules instead of incorporating with the binders, resulting in higher viscosity and lower workability for fresh mixtures [40]. As the fibre dosage rises to 4.8 kg/m^3, the flowability of the mixture is reduced by more than half, raising an issue when compacting concrete mixture. Hence, RTP fibre content of no higher than 4.8 kg/m^3 should be recommended to ensure the consistency of fresh mixtures, which is crucial for their hardened properties.

3.2 Weight loss

Fig. 5 presents the variations of weight loss with temperature for all mixtures, relative to their weights before heating. In general, the weight loss of the tested specimens increases when temperature rises. From 20 °C to 105 °C, the weight loss for all the specimens is almost the same (1% to 1.2% of the total weight), with only a tiny amount of free water evaporation. When temperature rises to 250 °C, the weight loss increases significantly to 6% for RTPF0 and 6.7% for RTPF48. This can be ascribed to the evaporation of physically absorbed water. In addition, the decomposition of the C-S-H structure takes place at this stage, which can lead to the release of chemically bound water from C-S-H gels [52]. At temperatures up to 400 °C, the effect of fibres on the weight loss of the specimens is pronounced. The weight loss increases from 6.2% to 7.1% with the increase of fibre content from 0 (RTPF0) to 4.8 kg/m^3 (RTPF48) at 400 °C. This can be attributed to further decomposition of C-S-H gels and the melting of RTP fibres, which reduce the bonding between RTP fibres and concrete while leaving some pores at the interfaces. Therefore, the interconnected pore network can be formed in the

8

RTP fibre reinforced specimens, which facilitates the evaporation of free water and the escape of vapour and thereby results in a relatively higher weight loss compared to the plain concrete. When the temperature reaches 600 °C, the weight loss values of RTPF0 and RTPF48 are found to be 8.5% and 9.2%, respectively. It is noteworthy that up to 600 °C, the weight loss of RTPF0 reaches 95.5% of the original water content prior to heating, which implies that most of the water in concrete is lost before the temperature exceeds 600 °C. This is consistent with the finding by other researchers that the primary change occurred in concrete was associated with the physically and chemically bound water at temperatures lower than 600 °C [18, 53-55].

3.3 Compressive strength

The compressive strength of concrete with various RTP fibre content is shown in Fig. 6. At ambient temperature, the incorporation of RTP fibres results in a reduction of compressive strength. The compressive strength is decreased by 12.8% with the increase of RTP fibre content from 0 to 4.8 kg/m^3. This tendency agrees well with the previous studies on RTP fibre reinforced concrete that the compressive strength of concrete was declined by 17.7% when the fibre content was increased from 0 to 9.6 kg/m^3 [32, 40]. This can be mainly attributed to two reasons: (1) The rubber granules inside the RTP fibres can cause an increase of entrained air content, which leads to the augment of porosity of the concrete specimen and thus lowers the compressive strength [40, 56]; (2) The interfaces between the rubber particles and concrete matrix are vulnerable to compressive loading, indicating a lower stiffness surrounding those rubber particles, which would promote the development of microcracks and thus accelerate the failure of concrete [57].

Fig. 7 illustrates the compressive strength of all specimens at elevated temperatures, where a downward trend can be observed when temperature rises. The compressive strength of RTPF0 is reduced from 47.5 MPa to 24.3 MPa while that of RTPF48 decreases from 41.4 MPa to 22.2 MPa when increasing the temperature from 20 °C to 600 °C. The control sample (RTPF0) has a compressive strength loss of 48.8% at 600 °C compared to that at ambient temperature. This is consistent with the previous finding that an average of 45% reduction of the plain concrete was observed at 600 °C [58]. In general, the compressive strength of all specimens decreases steadily by around 6.3% to 7.2% before 250 °C, due to the decomposition of C-S-H gels at around 105 °C that causes the strength loss as the C-S-H layers start to become unstable [52]. However, a sharp slope can be observed when the temperature exceeds 250 °C, implying that besides the desiccation of C-S-H gels within concrete, there are other reasons that accelerate the strength loss of specimens after 250 °C. It is worth noting that RTP fibres start to melt at 256 °C, which means the empty channels left by softening and melting of RTP fibres can increase the porosity of the specimen and consequently lower the compressive strength. In addition, when the temperature reaches 400 °C, concrete may suffer from the thermal incompatibility induced by the shrinkage of cement paste and

aggregate expansion that impairs the binding between these two phases. Moreover, the decrease of compressive strength can be associated with the decomposition of crystals (transformation of calcium hydroxide into calcium oxide and water) taken place at around 535 °C [52, 59].

Fig. 8 shows the relative compressive strength of all specimens to that obtained at ambient temperature. It can be observed that the relative compressive strength is almost identical from RTPF0 to RTPF48 when the temperature rises from 20 °C to 250 °C, which suggests that the compressive strength of concrete is barely affected by RTP fibre content before its melting at 256 °C. However, there exists an obvious difference at both 400 °C and 600 °C. As seen in Fig. 8, RTPF12 has the lowest relative compressive strength loss among all samples at 400 °C and 600 °C, which is 24.8% and 45.5%, respectively. This can be ascribed to the pores left by melting of RTP fibres, which increases the interconnected network to distribute pore pressure more uniformly. Other researchers also reported that the incorporation of polymer fibres could mitigate the deterioration of concrete after exposure to elevated temperatures to some extent [14], while the increase of porosity caused by fibre addition can negatively influence the compressive strength if the fibre content exceeds a certain amount, which explains the increase of strength loss from RTPF12 to RTPF48. In this case, the optimal RTP fibre content is suggested to be 1.2 kg/m^3 as RTPF12 shows the least relative compressive strength loss among all mixtures.

3.4 Ultrasonic pulse velocity

Fig. 9 demonstrates the UPV results of all mixtures. Overall, the UPV values can be considered as a great estimator of compressive strength of RTP fibre reinforced concrete exposed to elevated temperatures, since the UPV values decrease with the increase of elevated temperature, showing a similar trend to the compressive strength results. The ultrasonic speed of RTPF0 is reduced from around 4670 m/s to 1720 m/s when temperature rises from 20 °C to 600 °C. In general, the degradation of concrete microstructure is the main factor that affects the UPV values. The increase of porosity and entrained air content in concrete after exposure to elevated temperatures can enlarge the transport distance of ultrasonic wave and thus mitigate the transport speed [27, 60]. It is noted that the sharpest slope appears from 250 °C to 400 °C, which is consistent with the trend presented in Fig. 7 that the increase of gradient is observed when the temperature exceeds 250 °C. Moreover, the results indicate that RTPF12 has the highest UPV values of 2560 m/s and 2040 m/s at 400 °C and 600 °C, respectively, which also agrees well with the finding obtained from the compressive strength test that RTPF12 is the superior mixture compared to others.

3.5 Pore pressure

Fig. 10 shows the temperature development with heating time at different measuring points for an example specimen, i.e. RTPF12. Overall, the temperature increases with increasing heating time and reaches a plateau at the end. The highest temperature decreases from around 613 °C to 537 °C when

the measuring point is deeper away from the heated surface from 20 mm to 100 mm. For different mixtures, Fig. 11 displays a comparison of temperature change among all specimens at the same location, i.e. 50 mm from the heated surface. Obviously, all specimens show a similar tendency that the temperature increases constantly from 20 °C to 600 °C with a heating time of approximately 320 min, which indicates that the temperature evolution of concrete mixture is not sensitive to RTP fibre content. This is in good agreement with the previous work [42, 47, 61] that there was no significant influence of fibres on the concrete specimen temperature. That is because aggregates are the main contributor to overall thermal conductivity of concrete, rather than fibres in concrete. Since the same aggregates were used in all five mixtures, the thermal conductivity of them should be almost equivalent that results in the similar temperature evolution shown in Fig. 11.

Simultaneously, the pore pressure was measured for all mixtures at different locations. The pore pressure of an example specimen (RTPF12) at three locations was plotted as a function of temperature in Fig. 12. As it can be seen, the pore pressure increases with the augment of temperature until a peak pressure is reached. The peak pressure rises from 120 kPa to 395 kPa while the corresponding temperature declines from 344 °C to 255 °C, when the located measuring point is at 20 mm to 100 mm inside the heated surface. This reveals that the inner parts of the concrete specimen can experience a higher pore pressure at a relatively lower temperature compared to the heated surface. This can be ascribed to the migration of moisture from the heated surface inwards towards the low-temperature region, where the moisture and vapour accumulate to form a 'moisture clog' that impedes the vapour migration and thereby causes the pore pressure build-up [4]. It is noteworthy that based on the previous studies of plain concrete at elevated temperatures, greater pore pressure gradients were found within 20 mm from the heated surface than in the deeper zone of plain concrete [8, 50], whereas the results of the RTP fibre reinforced concrete specimens show that the pore pressure gradients are more significant at the inner parts, e.g., at 50 mm and 100 mm. This suggests that the existence of RTP fibres can influence the pore pressure build-up inside concrete matrix.

To estimate the influence of RTP fibre on pore pressure, the pore pressure evolution for the specimens with various RTP fibre content is investigated and presented in Fig. 13. It can be clearly observed that the increase of RTP fibre content can result in a mitigation of pore pressure in concrete when the temperature exceeds around 300 °C. At 350 °C, the pore pressure is reduced from 360 kPa to 46 kPa with increasing RTP fibre content from 0 to 4.8 kg/m^3, indicating a significant mitigation of approximately 87.2%. In addition, the pore pressure of RTPF0 and RTPF06 increases constantly when temperature rises, whereas others show a different tendency with a peak pressure observed in the curve. This is consistent with the previous study that the pore pressure of plain concrete sample was found to increase steadily at elevated temperatures [1], which can be attributed to the pore pressure build-up as it is difficult for vapour to escape from the dense structure of plain concrete. On

11

the other hand, the peak pore pressure decreases by approximately 68% when increasing the RTP fibre content from RTPF12 to RTPF 48, which implies that the addition of RTP fibre can effectively mitigate the pore pressure of concrete matrix. This can be ascribed to the increase of porosity and internal pore connectivity, allowing the vapour to be released from the existing and new pores induced by the melting of RTP fibres [2, 19, 23, 44, 47].

3.6 Microstructural evolution

3.6.1 Surface cracks

Fig. 14 displays the surface crack distribution of RTPF0 and RTPF24 after exposure to 400 °C and 600 °C in comparison with that at ambient temperature. There is no obvious surface crack for both RTPF0 and RTPF24 at ambient temperature. The amount of surface cracks increases with the rise of temperature, which can be ascribed to the increase of vapour pressure and thermal stresses when exposed to higher temperatures [38, 62]. The surface cracks are observed to have an improved connection with each other at 600 °C than that at 400 °C. At the same temperature, the surface cracks in RTPF24 are obviously less than those in RTPF0, which implies that the incorporation of RTP fibres can efficiently mitigate the surface cracking of concrete at elevated temperatures.

3.6.2 Thermal analysis

Fig. 15 shows the thermal analysis results in terms of DSC, TGA and DTG curves of RTPF0, RTPF12 and RTPF48. Similar tendencies of DSC, TGA and DTG curves can be found for all mixtures, suggesting that there is no crucial influence of incorporating RTP fibre on hydration products and change of free water inside concrete [9, 19]. The DSC curve presented in Fig. 15a reveals the heat transformation and the enthalpy change of concrete by measuring the heat flux to and from the specimen [26]. In this case, the DSC curve shows a sudden drop at around 100 °C corresponding to the free water evaporation and another one at 450 °C that represents the decomposition of hydration products, which is confirmed by other researchers that the decomposition of calcium hydroxide (CH) takes place between 450 °C and 520 °C [26].

Fig. 15b illustrates the TGA and DTG curves of concrete with various RTP fibre content. There exists a rapid decrease of the retained weight of all specimens from 60 °C to 200 °C due to the evaporation of physically and chemically bound water from C-S-H gels, which is the main contributor of total weight loss. Then, a fluctuation can be observed when the temperature reaches 450 °C, which can be attributed to the further vaporisation of chemically bound water that releases from the decomposition of calcium hydroxide.

3.6.3 Microstructure characteristics

Fig. 16 shows the XRD spectra of RTPF0 subjected to different temperatures, which indicate that the XRD spectra at 20, 105 and 250 °C is similar, whereas the loss of CH occurs between 400 °C and 600 °C, implying the decomposition of CH at high temperatures (> 400 °C). This is consistent with

the previous findings that the XRD spectra showed some fluctuations associated with the evaporation of free water, whereas no chemical changes were observed in concrete before 250 °C [9].

Fig. 17 presents the SEM images of RTPF48 at different temperatures. A representative region with some fibres is chosen to illustrate the microstructural evolution of RTP fibre reinforced concrete. At ambient temperature, a few microcracks can be observed around RTP fibres. The formation of cracks at this stage can be ascribed to the early-age shrinkage of concrete before and during curing. After exposing the specimen at 105 °C, new microcracks appear around RTP fibres, which can be attributed to the mismatch of expansion coefficients of RTP fibres and other matrix phases, i.e. mortar and aggregates [9]. Some microcracks induced by the surrounding fibres start to connect with others, as shown in Fig. 17b. When the temperature increases to 250 °C, the softening of RTP fibres can be identified in the SEM micrograph as it is close to the melting point at 256 °C. Meanwhile, some RTP fibres are partially disappeared from their channels. Moreover, the size and length of these microcracks tend to be greater with the occurrence of new microcracks in radial directions and the coalescent of them to form an interconnected network. At 400 °C and 600 °C, the existing cracks are found to grow in width, while some of the RTP fibres are completely disappeared with empty channels left. It is noteworthy that the pattern of interconnected network of RTP fibre reinforced specimen at 600 °C is comparatively similar to that at 105 °C, which suggests that the main contributor of the formation of microcrack network is the thermal incompatibility between different phases. This agrees well with the previous study that the thermal mismatch between fibres and concrete can be the most critical factor that affects the permeability of concrete at elevated temperatures [9]. However, as the microcracks initiate around the RTP fibre-matrix interface and propagate towards outside, the empty channels left by RTP fibres at 400 °C and 600 °C become spontaneously connected with each other to form a pore-microcrack combined network.

3.6.4 Pore structure

The pore size distribution and cumulative pore volume of all five mixtures at ambient temperature (20 °C) and 600 °C are shown in Figs. 18 and 19, respectively. At 20 °C, the pore size with the largest volume fraction grows from 0.0324 µm to 0.0403 µm when the fire content increases from 0 (RTPF0) to 1.2 kg/m³ (RTPF12), with a difference of approximately 24.4%. This reveals that the incorporation of RTP fibres can result in a lower density of concrete matrix by inducing larger pores in the system. At ambient temperature, the highest porosity is found in RTPF48, which is about 66.6% higher than that of the plain specimen, which implies that the addition of RTP fibres can cause an augment of total porosity of concrete at ambient temperature. At 600 °C, the pore size with the largest volume fraction increases significantly from 0.0403 µm to 0.0954 µm with the increase of RTP fibre content from 0 to 2.4 kg/m³, while a lower value of 0.0403 µm can be found when increasing the fibre content to 4.8 kg/m³. Compared to RTPF0, the total porosity of RTPF06 and RTPF12 is increased by 39.2%

13

and 12.6%, respectively, but reduced by approximately 10.6% and 15.4% at a fibre dosage of 2.4 kg/m^3 and 4.8 kg/m^3, respectively. This is can be explained by the fact that when the fibre content exceeds a certain level some residual fibres may exist inside concrete and consequently lower the total porosity of concrete at high temperatures.

4. Discussion

4.1 Mechanism of concrete damage at elevated temperatures

Herein, further analyses of the above-mentioned experimental results in terms of thermal and mechanical properties and microstructural characteristics of concrete at different temperatures were carried out to better understand the mechanism of concrete damage at elevated temperatures. In general, damage evolution in concrete at elevated temperatures is associated with physicochemical changes and transport of water and vapour within concrete, as illustrated in Fig. 20.

Based on the weight loss, DSC and TGA results, the physicochemical changes of concrete at elevated temperatures can be demonstrated at three temperature levels: (1) *Level I* (up to 105 °C) corresponding to the free and physically bound water evaporation; (2) *Level II* (105 °C to 400 °C) associated with the decomposition of C-S-H gels which releases chemically bound water; and (3) *Level III* (400 °C to 600 °C) related to the decomposition of CH gels. The conceptual illustration is given in Fig. 20a.

At *Level I*, there was only loss of free and physically bound water as concrete dried out since no hydrothermal reactions occurred based on the thermal analysis and XRD spectra. According to the weight loss and strength measurement, the evaporated water at this stage accounted for about 14% of the total weight loss and 3% of the compressive strength loss. At *Level II*, the chemically bound water was released from C-S-H gels and the structure became unstable. The largest weight loss took place at this stage, which was around 70% of the total weight loss. Due to the dehydration of C-S-H gels, the compressive strength of concrete was significantly reduced by approximately 26% of the original strength at *Level II*. In addition, the XRD results showed that CH gels disappeared between 400 °C and 600 °C, implying the decomposition of calcium hydroxide when temperature exceeded 400 °C. Apparently, the DSC curve corroborated the previous findings that the heat flux had a sudden drop starting from around 400 °C and reached a peak at about 450 °C, which also reveals the decomposition of calcium hydroxide. This led the concrete damage to *Level III* where calcium hydroxide was decomposed to calcium oxide and water. Due to high temperature at *Level III*, the water became vapour immediately, which escaped from concrete through the interconnected pore network. The TGA curve also showed a sudden drop at this stage, representing the vaporisation of chemically bound water in calcium hydroxide. The compressive strength loss at this stage can be attributed to both the dissociation of Portlandite (CH) and further decomposition of C-S-H gels, which was found to be about 20% of the compressive strength at ambient temperature with a weight loss of 16% in

14

comparison with the total weight loss. The previous efforts also reported that the weight loss and mitigation of concrete strength can be ascribed to the decomposition of hydration products, i.e. C-S-H and CH gels [9, 63, 64].

On the other hand, transport of water and vapour at elevated temperatures could also cause damage inside concrete. During the water vaporisation and migration process, moisture and vapour might not only move outwards towards the heated surface of concrete but also inwards towards the internal matrix [8, 65]. Therefore, the damage could be induced as moisture moved through pores, which was recognised as pore pressure induced damage. This type of damage can be attributed to the increase of pore pressure induced stress, resulting from the expansion of air and condensed moisture under high temperatures within the non-deformable pore structure. As seen in Fig. 13, the pore pressure of RTPF0 continuously increased as temperature rose, suggesting that the pore pressure kept building up until a threshold point was reached. The cracks would then develop in a violent way with the energy released from the pores that was saturated by vapour pressure, leading to the damage of concrete in an explosive manner in terms of the aforementioned compressive strength and UPV values [8]. Hence, to prevent the build-up of pore pressure to a limit value that causes damage of concrete, RTP fibres were applied to improve the transport of moisture and thus reduce the pore pressure in concrete.

4.2 Mechanism of RTP fibres in mitigating concrete damage at elevated temperatures

The main purpose of adding RTP fibres to concrete is to minimise the pore pressure induced damage and thus mitigate the damage of concrete at elevated temperatures. The thermal analysis and XRD results of RTP fibre reinforced concrete at elevated temperatures indicated that the presence of RTP fibres did not affect the hydrothermal reactions (i.e. decomposition of C-S-H and CH gels) taken place in comparison with the plain concrete. This was also confirmed by the previous study that polymer fibres had no influence on hydration products of concrete [9]. Therefore, the effect of RTP fibres on behaviour of concrete at elevated temperatures was further investigated based on microstructural analysis. As seen in the pore size distribution, the addition of RTP fibres could lead to an increase of the volume fraction of larger pores compared to the plain concrete at ambient temperature, which lowered the density of concrete.

Different from the plain concrete, one more critical temperature point, i.e. the melting point of RTP fibres of 256 °C should be considered for the specimens with RTP fibres, as the melting of RTP fibres could eventually change the microstructure of concrete. This was supported by the SEM images shown in Fig. 17 that on one hand the softening of fibres caused some gaps between the original channel and fibres themselves and, on the other hand, the thermal mismatch between RTP fibres and concrete matrix resulted in the initiation of microcracks which propagated along the radial direction of fibre's cross section [4]. They both contributed to improving the internal pore connectivity of

15

concrete, and thus released the trapped moisture to prevent pore pressure build-up. Consequently, the pore pressure of RTP fibre reinforced concrete specimens (RTPF12, RTPF24 and RTPF48) showed a peak point followed by a decline as the temperature rose (see Fig. 13). Fig. 20b shows a schematic illustration of the microstructural changes of RTP fibre reinforced concrete at elevated temperatures. When the temperature reached 400 °C and 600 °C, the empty channels can be observed as RTP fibres melted completely. The channels left by fibres were well connected with the microcracks around them, which could further facilitate the interconnected network to relieve vapour pressure. Hence, the higher the fibre content was used, the better the internal pore connectivity and the lower peak pore pressure was reached. Consequently, the pore pressure induced damage of concrete under high temperatures can be mitigated. However, the increase of fibre content could also negatively affect the mechanical properties of concrete, as too large crack density and number of empty channels could result in a reduction of compressive strength. Also, if the fibre content is too high, some of the fibres might be left halfway inside the channels, which could potentially impede the transport of water and vapour as explained previously. Therefore, an appropriate amount of RTP fibres should be included in the mixture, which was found to be 1.2 kg/m^3 in this study, considering both strength and pore pressure in accordance to the experimental results.

In literature, the addition of PP fibres was considered as an effective measure to mitigate the pore pressure induced damage in concrete at elevated temperatures [4, 19]. It was found that PP fibres expanded significantly at elevated temperatures with a 10 times larger coefficient of thermal expansion compared to concrete [4]. This essential thermal incompatibility led to the formation of multiple microcracks, which promoted the interconnection between pores and microcracks and thus reduced the pore pressure induced stress. Whereas, RTP fibres experienced both expansion and softening at elevated temperatures, which also enhanced the interconnected pore network of concrete. Both approaches could effectively mitigate the high temperature-induced damage of concrete before and after the melting of fibres. Regarding the mitigation methods, as stated in the previous study, besides requiring a significant thermal mismatch with the concrete matrix, the aspect ratio of fibres should be large enough to have a great number density of dispersed particles in concrete [9]. It is convenient to control the aspect ratio of PP fibres as they are manufactured products, but it might be difficult for RTP fibres as they are recycled from waste tyres and have a wide range of size distribution. Further investigation will be needed to find out an efficient approach to practically sieve RTP fibres in terms of different aspect ratios. Nevertheless, RTP fibres as a sustainable and promising alternative to PP fibres can help effectively mitigate the damage of concrete at elevated temperatures.

5. Conclusions

This study presents a systematic investigation on the behaviour of recycled tyre polymer (RTP) fibre reinforced concrete at elevated temperatures (20, 105, 250, 400 and 600 °C). A series of tests

16

including slump, uniaxial compression, pore pressure, ultrasonic pulse velocity (UPV), differential scanning calorimeter (DSC), thermogravimetric analysis (TGA), X-ray diffractometer (XRD), scanning electron microscope (SEM) and mercury intrusion porosimetry (MIP) were conducted to explore the properties and microstructural characteristics of concrete with various RTP fibre content (0, 0.6, 1.2, 2.4 and 4.8 kg/m^3 corresponding to 0%, 0.05%, 0.1%, 0.2% and 0.4% V_f) subjected to elevated temperatures. According to the experimental results, the main conclusions can be drawn as follows:

- The addition of RTP fibres caused a decrease of workability by up to 51.5% at ambient temperature (20 °C), which can be ascribed to the increased shear resistance. The compressive strength was reduced by 12.8% with increasing RTP fibre content from 0 to 4.8 kg/m^3 at 20 °C and by around 45.5% at 600 °C when adding 1.2 kg/m^3 RTP fibres.

- The physicochemical process of RTP fibre reinforced concrete can be summarised by three critical temperatures: free water vaporisation and decomposition of C-S-H gels at 105 °C; melting of RTP fibres at 256 °C; and decomposition of calcium hydroxide at 400 °C.

- The incorporation of RTP fibres can effectively mitigate the pore pressure of concrete at elevated temperatures, as the melting of RTP fibres left empty channels for vapour release which were well connected to the microcracks induced by thermal mismatch between RTP fibres and concrete. Consequently, the internal pore/crack connectivity of concrete was increased, which impeded the pore pressure built-up in concrete at high temperatures. The pore pressure of plain concrete continuously built up with the increase of temperature, while there existed a peak pore pressure in RTP fibre reinforced concrete with fibre content $\geq$ 1.2 kg/m^3, which was decreased by 68% as the RTP fibre content increased from 1.2 kg/m^3 (RTPF12) to 4.8 kg/m^3 (RTPF48).

- The pore structure of concrete at elevated temperatures was significantly influenced by RTP fibre content. At 600 °C, the total porosity of concrete was increased by 39.2% at a fibre dosage of 0.6 kg/m^3 (RTPF06), whereas a decrease in porosity by up to 15.4% (RTPF48) could happen if the RTP fibre content is too high since there might be residual fibres left in concrete at higher temperatures and thus lowered the porosity of concrete. The optimal RTP fibre content was found to be 1.2 kg/m^3 considering the fresh and hardened properties and effectiveness of RTP fibres in mitigating high temperature-induced damage of concrete.

The experimental study on behaviour of RTP fibre reinforced concrete at elevated temperatures indicated that RTP fibres can be considered as a promising sustainable alternative to manufactured polymer fibres for mitigating damage of concrete subjected to elevated temperatures. Herein, only the static mechanical properties of RTP fibre reinforced concrete at elevated temperatures were investigated, while the effect of RTP fibres on dynamic mechanical properties of concrete exposed to elevated temperatures remains unknown. For a wide range of practical applications, it is vital to

explore the coupled effect of temperature and strain rate on dynamic mechanical properties of RTP fibre reinforced concrete in comparison with commonly used polymer fibres such as PP, PVA and PE [27, 40, 66, 67]. This is a subject of ongoing work and will be presented in a future publication.

Acknowledgements

References

[1] J.C. Mindeguia, P. Pimienta, A. Noumowe, M. Kanema, Temperature, pore pressure and mass variation of concrete subjected to high temperature - Experimental and numerical discussion on spalling risk, Cement Concrete Res, 40 (2010) 477-487.

[2] Y. Li, P. Pimienta, N. Pinoteau, K.H. Tan, Effect of aggregate size and inclusion of polypropylene and steel fibers on explosive spalling and pore pressure in ultra-high-performance concrete (UHPC) at elevated temperature, Cement Concrete Comp, 99 (2019) 62-71.

[3] A.A. Stec, K. Dickens, J.L. Barnes, C. Bedford, Environmental contamination following the Grenfell Tower fire, Chemosphere, 226 (2019) 576-586.

[4] Y. Li, K.H. Tan, E.H. Yang, Synergistic effects of hybrid polypropylene and steel fibers on explosive spalling prevention of ultra-high performance concrete at elevated temperature, Cement Concrete Comp, 96 (2019) 174-181.

[5] E.W. Klingsch, Explosive spalling of concrete in fire, IBK Bericht, 356 (2014) 17-39.

[6] V.K.R. Kodur, L. Phan, Critical factors governing the fire performance of high strength concrete systems, Fire Safety J, 42 (2007) 482-488.

[7] Q. Ma, R. Guo, Z. Zhao, Z. Lin, K. He, Mechanical properties of concrete at high temperature—A review, Constr Build Mater, 93 (2015) 371-383.

[8] Y. Li, Material properties and explosive spalling of ultra-high performance concrete in fire, Doctoral dissertation, Nanyang Technological University, 2018, pp.13-59.

[9] D. Zhang, A. Dasari, K.H. Tan, On the mechanism of prevention of explosive spalling in ultra-high performance concrete with polymer fibers, Cement Concrete Res, 113 (2018) 169-177.

[10] Z.P. Baiant, B. IO Analysis of Pore Pressure, Thermal Stress and Fracture in Rapidly Heated Concrete, International Workshop on Fire Performance of High Strength Concrete, NIST SP 919, Gaithersburg, MD, 1997, pp.155-164.

[11] X.W. Liang, C.Q. Wu, Y. Su, Z. Chen, Z.X. Li, Development of ultra-high performance concrete with high fire resistance, Constr Build Mater, 179 (2018) 400-412.

[12] Y. Su, C. Wu, J. Li, Z.X. Li, W. Li, Development of novel ultra-high performance concrete: From material to structure, Constr Build Mater, 135 (2017) 517-528.

[13] Y. Chan, X. Luo, W. Sun, Compressive strength and pore structure of high-performance concrete after exposure to high temperature up to 800 ºC, Cement Concrete Res, 30 (2000) 247-251.

[14] C. Bing, J.Y. Liu, Residual strength of hybrid-fiber-reinforced high-strength concrete after exposure to high temperatures, Cement Concrete Res, 34 (2004) 1065-1069.

[15] R. Ranade, V.C. Li, M.D. Stults, W.F. Heard, T.S. Rushing, Composite properties of high-strength, high-ductility concrete, Aci Mater J, 110 (2013) 413-422.

[16] Y.S. Heo, J.G. Sanjayan, C.G. Han, M.C. Han, Critical parameters of nylon and other fibres for spalling protection of high strength concrete in fire, Mater Struct, 44 (2011) 599-610.

[17] H. Wu, X. Lin, A. Zhou, A review of mechanical properties of fibre reinforced concrete at elevated temperatures, Cement Concrete Res, 135 (2020) 106117.

[18] A.A. Deshpande, D. Kumar, R. Ranade, Influence of high temperatures on the residual mechanical properties of a hybrid fiber-reinforced strain-hardening cementitious composite, Constr Build Mater, 208 (2019) 283-295.

[19] M.R. Bangi, T. Horiguchi, Pore pressure development in hybrid fibre-reinforced high strength concrete at elevated temperatures, Cement Concrete Res, 41 (2011) 1150-1156.

[20] P. Pliya, A.L. Beaucour, A. Noumowe, Contribution of cocktail of polypropylene and steel fibres in improving the behaviour of high strength concrete subjected to high temperature, Constr Build Mater, 25 (2011) 1926-1934.

[21] J.C. Liu, K.H. Tan, Mechanism of PVA fibers in mitigating explosive spalling of engineered cementitious composite at elevated temperature, Cement Concrete Comp, 93 (2018) 235-245.

[22] A.H. Akca, N.O. Zihnioglu, High performance concrete under elevated temperatures, Constr Build Mater, 44 (2013) 317-328.

[23] W. Khaliq, V. Kodur, Effectiveness of Polypropylene and Steel Fibers in Enhancing Fire Resistance of High-Strength Concrete Columns, J Struct Eng, 144 (2018) 04017224.

[24] V. Kodur, Spalling in high strength concrete exposed to fire: concerns, causes, critical parameters and cures, Adv Struct Eng , 2000, pp. 1-9.

[25] E. Rudnik, T. Drzymala, Thermal behavior of polypropylene fiber-reinforced concrete at elevated temperatures, J Therm Anal Calorim, 131 (2018) 1005-1015.

[26] A. Noumowe, Mechanical properties and microstructure of high strength concrete containing polypropylene fibres exposed to temperatures up to 200 C, Cement Concrete Res, 35 (2005) 2192-2198.

[27] M. Chen, H. Zhong, M. Zhang, Flexural fatigue behaviour of recycled tyre polymer fibre reinforced concrete, Cement Concrete Comp, 105 (2020) 103441.

[28] O. Onuaguluchi, N. Banthia, Scrap tire steel fiber as a substitute for commercial steel fiber in cement mortar: Engineering properties and cost-benefit analyses, Resour Conserv Recy, 134 (2018) 248-256.

[29] K. Adalberth, Energy use during the life cycle of single-unit dwellings: Examples, Build Environ, 32 (1997) 321-329.

[30] H. Zhong, E.W. Poon, K. Chen, M. Zhang, Engineering properties of crumb rubber alkali-activated mortar reinforced with recycled steel fibres, J Clean Prod, 238 (2019) 117950.

[31] S.S. Huang, H. Angelakopoulos, K. Pilakoutas, I. Burgess, Reused Tyre Polymer Fibre for Fire-Spalling Mitigation, Appl Struct Fire Eng, 2016.

[32] A. Baricevic, M.J. Rukavina, M. Pezer, N. Stirmer, Influence of recycled tire polymer fibers on concrete properties, Cement Concrete Comp, 91 (2018) 29-41.

[33] G. Marmol, S.F. Santos, H. Savastano, M.V. Borrachero, J. Monzo, J. Paya, Mechanical and physical performance of low alkalinity cementitious composites reinforced with recycled cellulosic fibres pulp from cement kraft bags, Ind Crop Prod, 49 (2013) 422-427.

[34] A. Baricevic, M. Pezer, M.J. Rukavina, M. Serdar, N. Stirmer, Effect of polymer fibers recycled from waste tires on properties of wet-sprayed concrete, Constr Build Mater, 176 (2018) 135-144.

[35] M. Serdar, A. Baricevic, M.J. Rukavina, M. Pezer, D. Bjegovic, N. Stirmer, Shrinkage Behaviour of Fibre Reinforced Concrete with Recycled Tyre Polymer Fibres, Int J Polym Sci, (2015) 145918.

[36] Y. Li, S. Huang, K. Pilakoutas, H. Angelakopoulos, I. Burgess, Mitigation of fire-induced spalling of concrete using recycled tyre polymer fibre, Proceedings of the 6th International Workshop on Concrete Spalling due to Fire Exposure, Sheffield, UK, 2019, pp. 19-20.

[37] F.P. Figueiredo, S.S. Huang, H. Angelakopoulos, K. Pilakoutas, I. Burgess, Effects of recycled steel and polymer fibres on explosive fire spalling of concrete, Fire Technol, 55 (2019) 1495-1516.

[38] F.P. Figueiredo, A.H. Shah, S.S. Huang, H. Angelakopoulos, K. Pilakoutas, I. Burgess, Fire protection of concrete tunnel linings with waste tyre fibres, Procedia Eng, 210 (2017) 472-478.

[39] GB/T 175-2007, Common Portland Cement, Chinese national standard, 2007.

[40] M. Chen, W. Chen, H. Zhong, D. Chi, Y. Wang, M. Zhang, Experimental study on dynamic compressive behaviour of recycled tyre polymer fibre reinforced concrete, Cement Concrete Comp, 98 (2019) 95-112.

[41] GB/T21120-2007, Synthetic Fibres for Cement, Cement Mortar and Concrete, Chinese national standard, 2007.

[42] P. Kalifa, G. Chene, C. Galle, High-temperature behaviour of HPC with polypropylene fibres: From spalling to microstructure, Cement Concrete Res, 31 (2001) 1487-1499.

[43] Y.S. Heo, J.G. Sanjayan, C.G. Han, M.C. Han, Synergistic effect of combined fibers for spalling protection of concrete in fire, Cement Concrete Res, 40 (2010) 1547-1554.

[44] Y.N. Ding, C. Zhang, M.L. Cao, Y.L. Zhang, C. Azevedo, Influence of different fibers on the change of pore pressure of self-consolidating concrete exposed to fire, Constr Build Mater, 113 (2016) 456-469.

[45] M. Ezziane, L. Molez, R. Jauberthie, D. Rangeard, Heat exposure tests on various types of fibre mortar, Eur J Environ Civ En, 15 (2011) 715-726.

[46] X. Liang, C. Wu, Y. Yang, Z. Li, Experimental study on ultra-high performance concrete with high fire resistance under simultaneous effect of elevated temperature and impact loading, Cement Concrete Comp, 98 (2019) 29-38.

[47] M.R. Bangi, T. Horiguchi, Effect of fibre type and geometry on maximum pore pressures in fibre-reinforced high strength concrete at elevated temperatures, Cement Concrete Res, 42 (2012) 459-466.

[48] GB/T50080-2016, Testing Methods of Workability of Normal Concrete, China Building Materials Academy, 2016.

[49] GB/T50081-2002, Testing Methods of Mechanical Properties of Normal Concrete, China Building Materials Academy, 2002.

[50] P. Kalifa, F.D. Menneteau, D. Quenard, Spalling and pore pressure in HPC at high temperatures, Cement Concrete Res, 30 (2000) 1915-1927.

[51] G. Fang, H. Bahrami, M. Zhang, Mechanisms of autogenous shrinkage of alkali-activated fly ash-slag pastes cured at ambient temperature within 24 h, Constr Build Mater, 171 (2018) 377-387.

[52] K.D. Hertz, Concrete strength for fire safety design, Mag Concrete Res, 57 (2005) 445-453.

[53] J.Z. Xiao, H. Falkner, On residual strength of high-performance concrete with and without polypropylene fibres at elevated temperatures, Fire Safety J, 41 (2006) 115-121.

[54] L.T. Phan, J.R. Lawson, F.L. Davis, Effects of elevated temperature exposure on heating characteristics, spalling, and residual properties of high performance concrete, Mater Struct, 34 (2001) 83-91.

[55] M. Sahmaran, M. Lachemi, V.C. Li, Assessing Mechanical Properties and Microstructure of Fire-Damaged Engineered Cementitious Composites, Aci Mater J, 107 (2010) 297-304.

[56] A. Benazzouk, O. Douzane, K. Mezreb, M. Queneudec, Physico-mechanical properties of aerated cement composites containing shredded rubber waste, Cement Concrete Comp, 28 (2006) 650-657.

[57] B.S. Thomas, R.C. Gupta, A comprehensive review on the applications of waste tire rubber in cement concrete, Renew Sust Energ Rev, 54 (2016) 1323-1333.

[58] C. Poon, Z. Shui, L. Lam, Compressive behavior of fiber reinforced high-performance concrete subjected to elevated temperatures, Cement Concrete Res, 34 (2004) 2215-2222.

[59] N.V.S. Kumar, K.S.S. Ram, Performance Of Concrete At Elevated Temperatures Made With Crushed Rock Dust As Filler Material, Mater Today-Proc, 18 (2019) 2270-2278.

[60] S.A. Omer, R. Demirboga, W.H. Khushefati, Relationship between compressive strength and UPV of GGBFS based geopolymer mortars exposed to elevated temperatures, Constr Build Mater, 94 (2015) 189-195.

[61] W. Khaliq, V. Kodur, Thermal and mechanical properties of fiber reinforced high performance self-consolidating concrete at elevated temperatures, Cement Concrete Res, 41 (2011) 1112-1122.

[62] Y. Li, Y. Zhang, E.H. Yang, K.H. Tan, Effects of geometry and fraction of polypropylene fibers on permeability of ultra-high performance concrete after heat exposure, Cement Concrete Res, 116 (2019) 168-178.

[63] S.M. Park, J.G. Jang, N. Lee, H.K. Lee, Physicochemical properties of binder gel in alkali-activated fly ash/slag exposed to high temperatures, Cement Concrete Res, 89 (2016) 72-79.

[64] O.G. Rivera, W.R. Long, C.A. Weiss, R.D. Moser, B.A. Williams, K. Torres-Cancel, E.R. Gore, P.G. Allison, Effect of elevated temperature on alkali-activated geopolymeric binders compared to portland cement-based binders, Cement Concrete Res, 90 (2016) 43-51.

[65] H.Y. Chu, J.Y. Jiang, W. Sun, M. Zhang, Thermal behavior of siliceous and ferro-siliceous sacrificial concrete subjected to elevated temperatures, Mater Design, 95 (2016) 470-480.

[66] M. Chen, H. Zhong, H. Wang, M. Zhang, Behaviour of recycled tyre polymer fibre reinforced concrete under dynamic splitting tension, Cement Concrete Comp, 114 (2020) 103764.

[67] H. Zhong, M. Zhang, Effect of recycled tyre polymer fibre on engineering properties of sustainable strain hardening geopolymer composites, Cement Concrete Comp, 122 (2021) 104167.
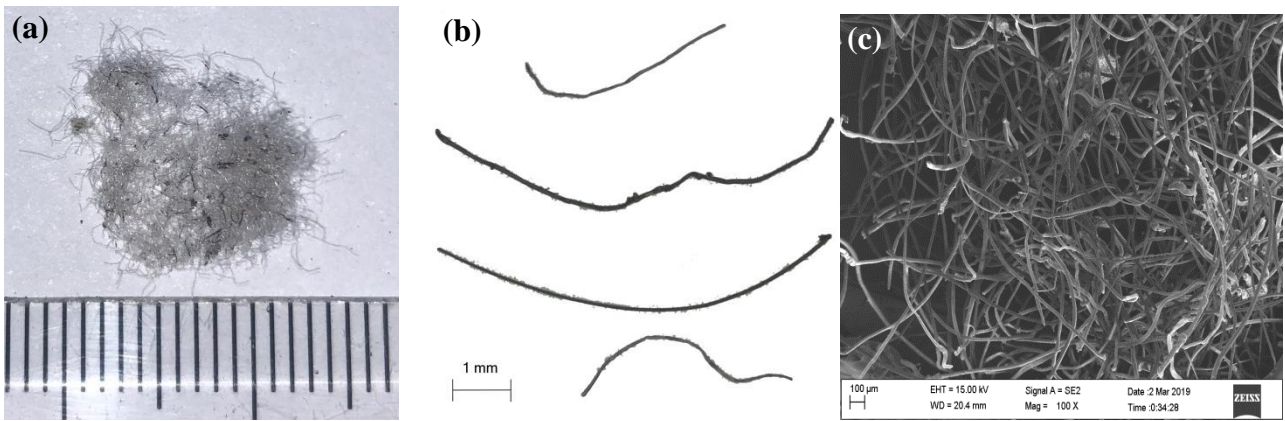
Fig. 1. RTP fibre used in this study: (a) picture of RTP fibre; (b) RTP fibre under microscope; (c) SEM image of RTP fibre.
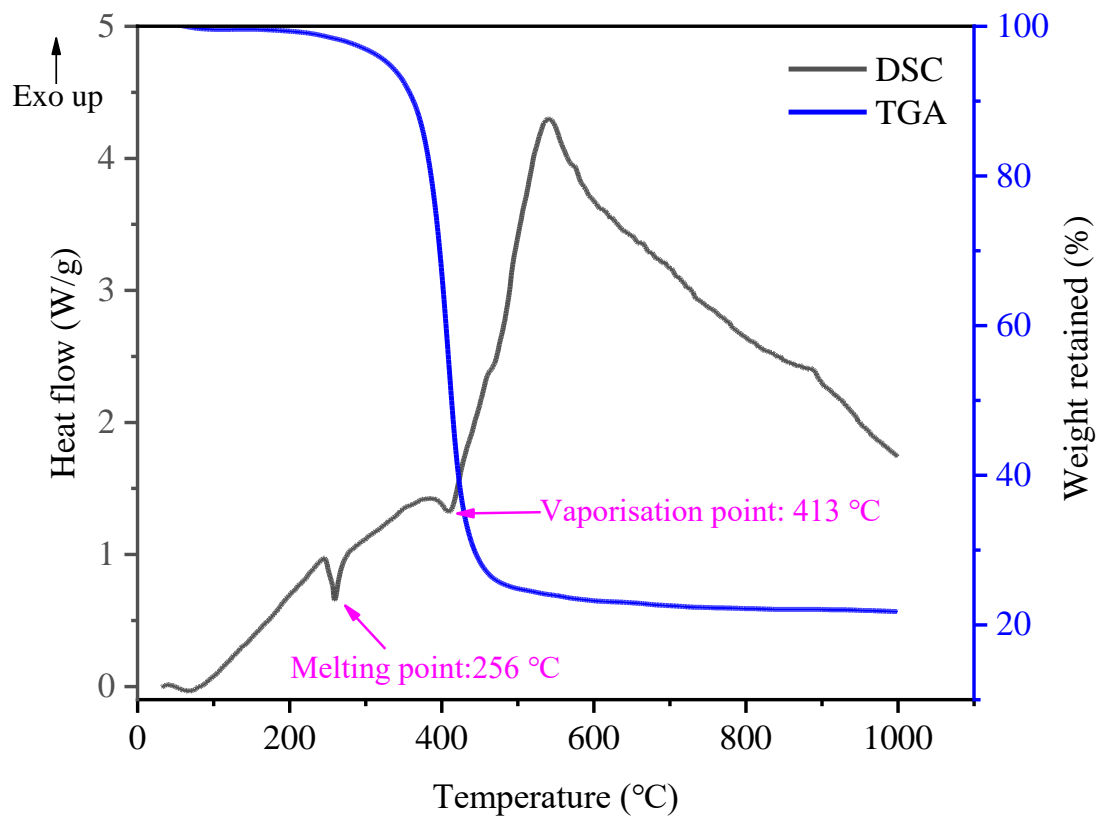
Fig. 2. DSC and TGA curves of RTP fibre.
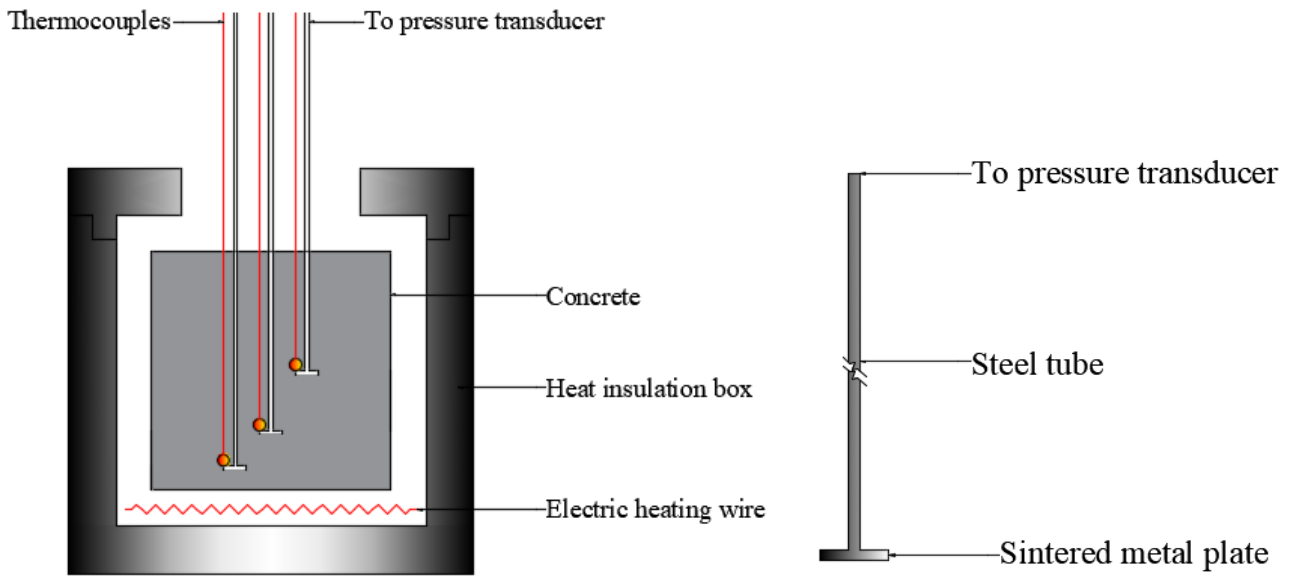
Fig. 3. Pore pressure test setup.
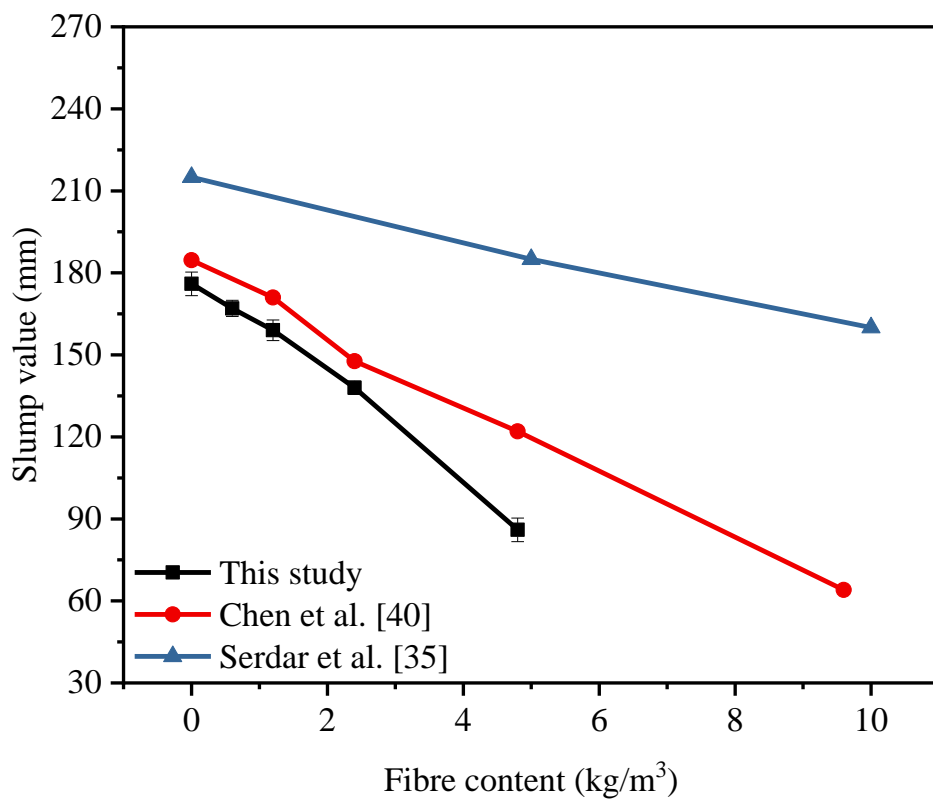
Fig. 4. Slump values of concrete with various fibre content.
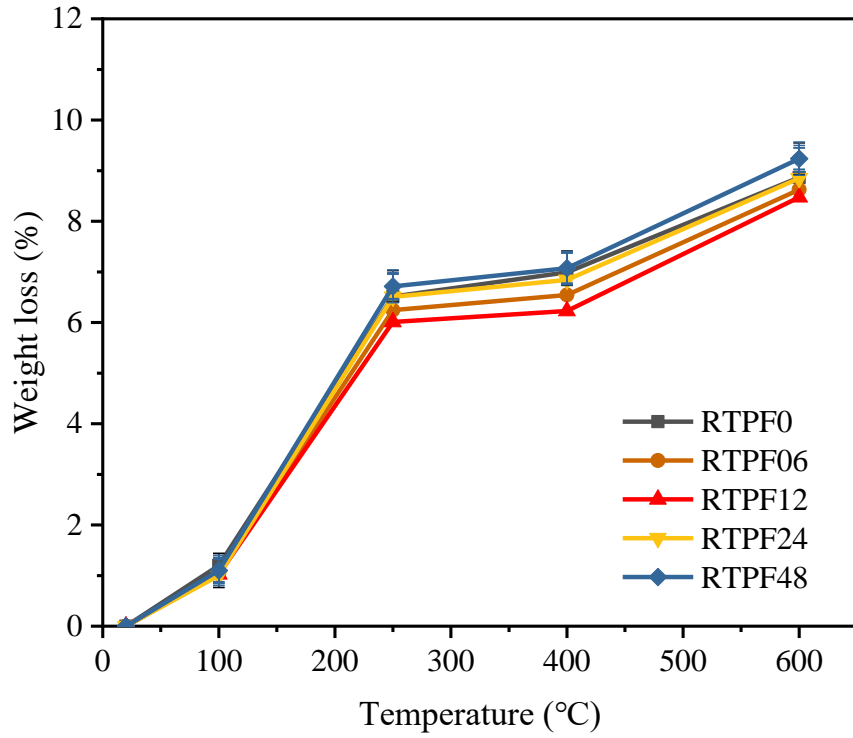
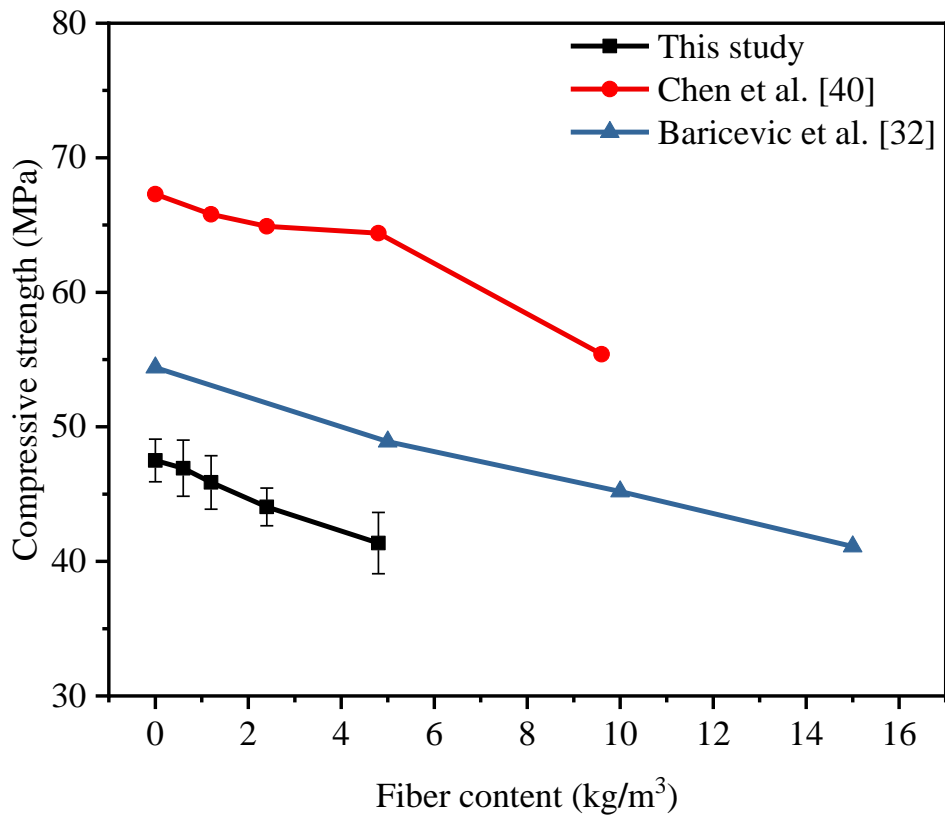Fig. 5. Weight loss of specimens with various RTP fibre con tent at elevated temperatures.

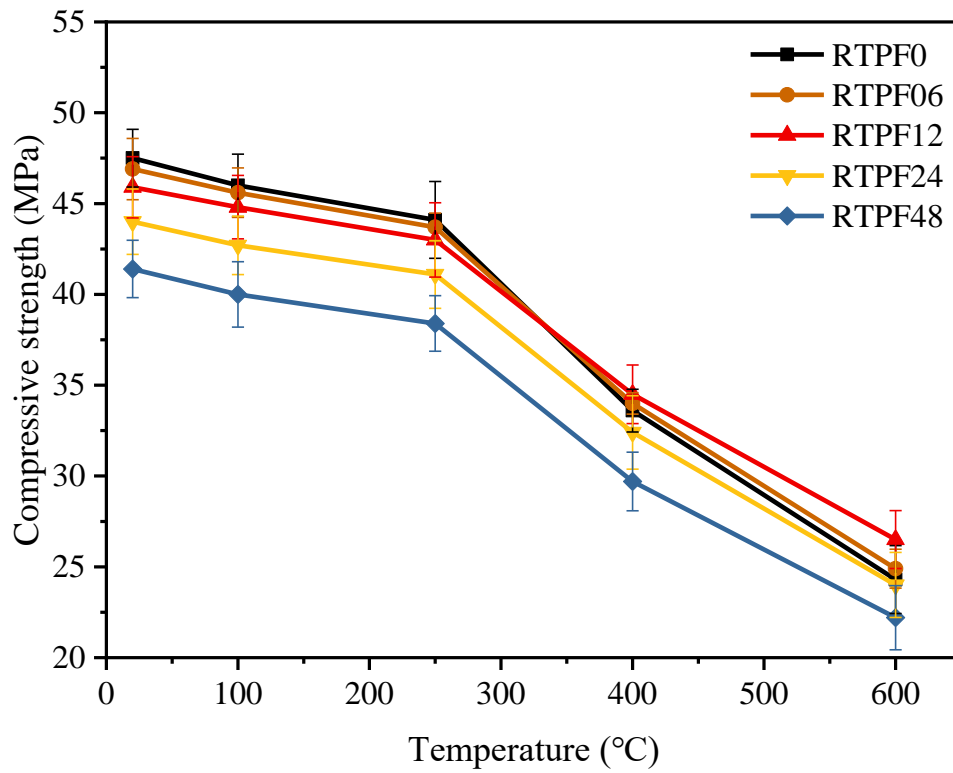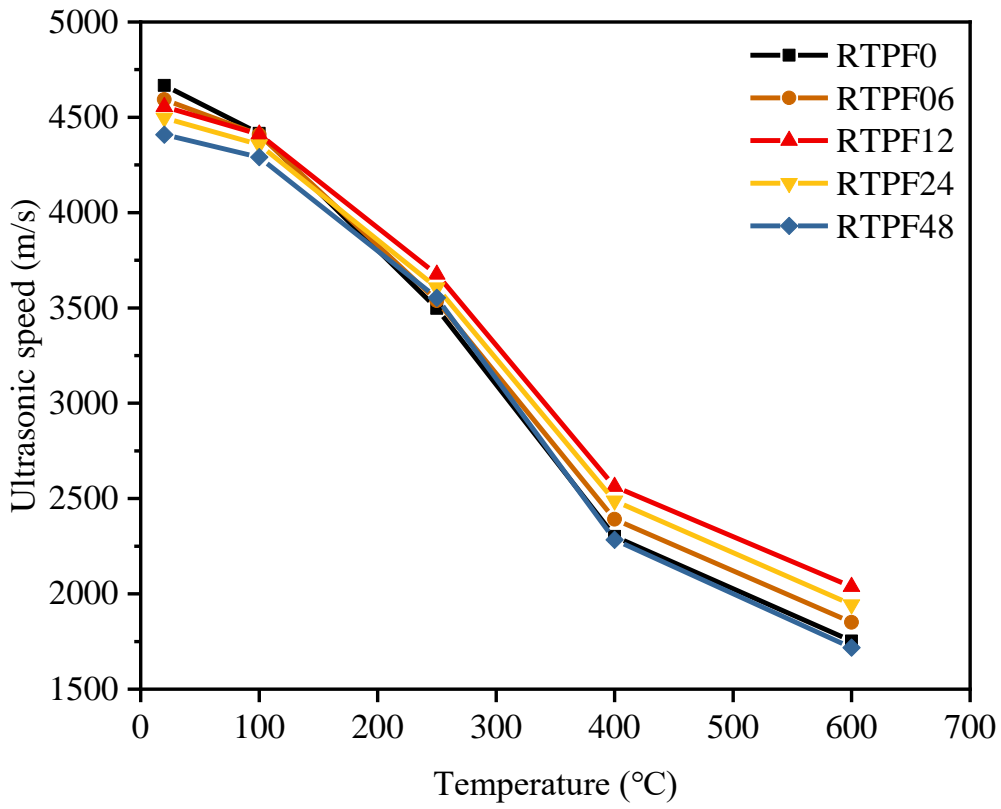Fig. 6. Compressive strength of concrete with various RTP fibre content.

Fig. 7. Compressive strength of concrete with various RTP fibre content at elevated temperatures.
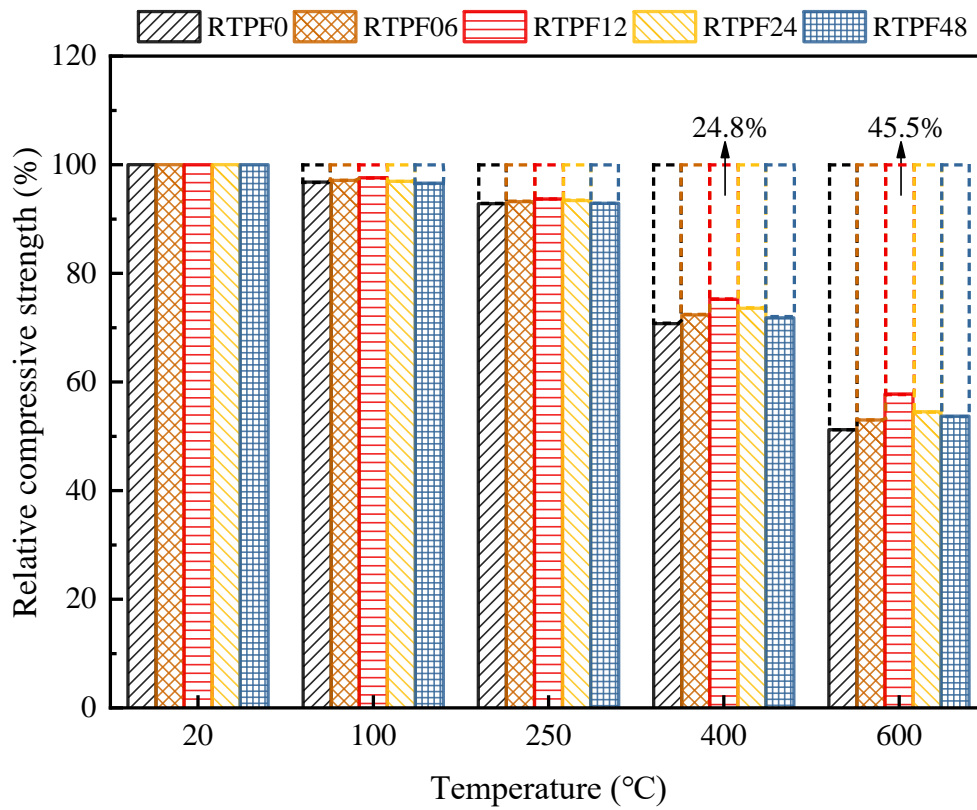
Fig. 8. Relative strength of concrete with various RTP fibre content at elevated temperatures.

Fig. 9. UPV value of concrete with various RTP fibre content at elevated temperatures.
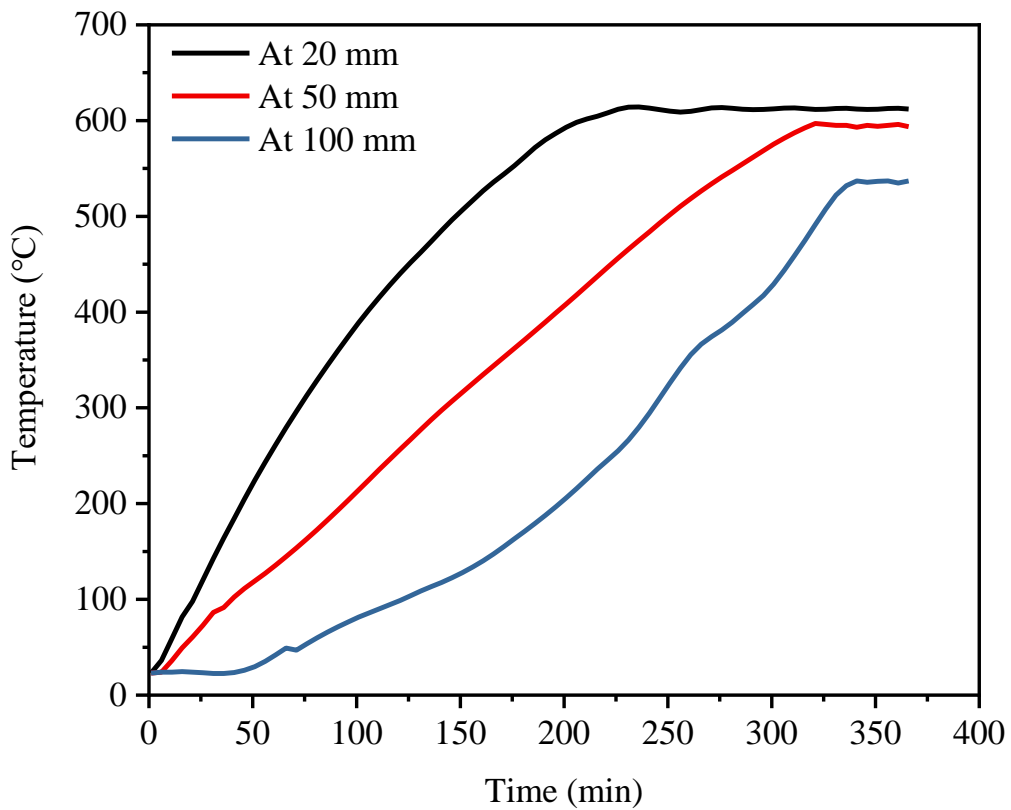
Fig. 10. Temperature evolution of specimen RTPF12 at 20, 50 and 100 mm from the heated face.
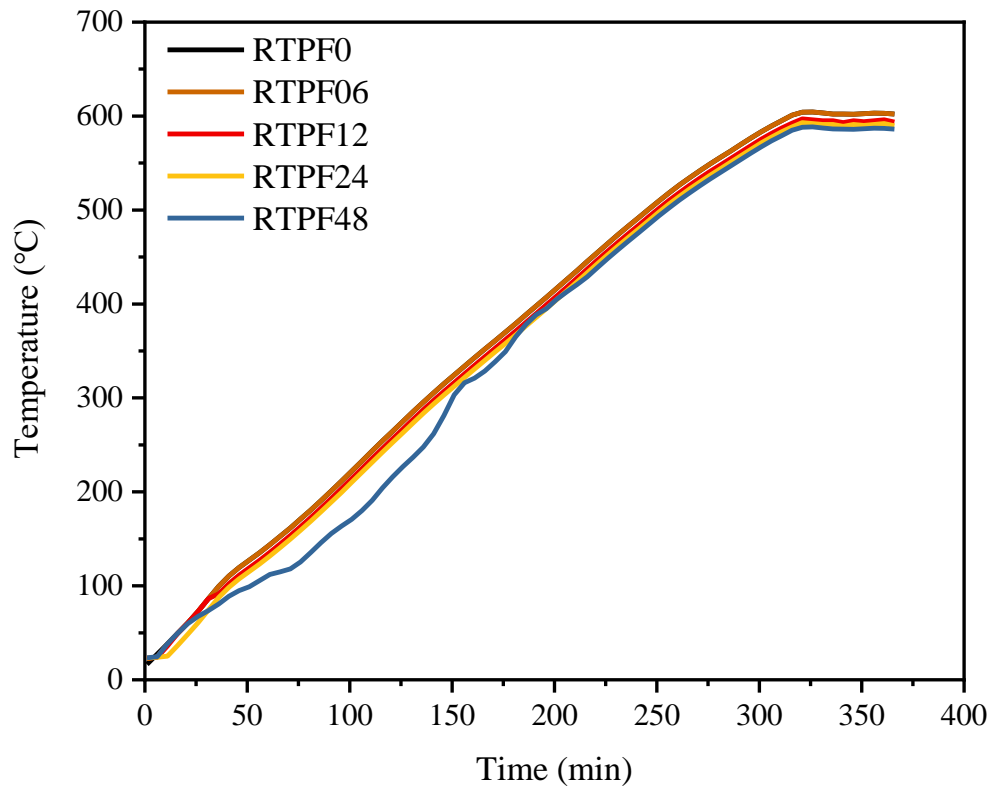
Fig. 11. Temperature evolution of concrete with various RTP fibre content at 50 mm.
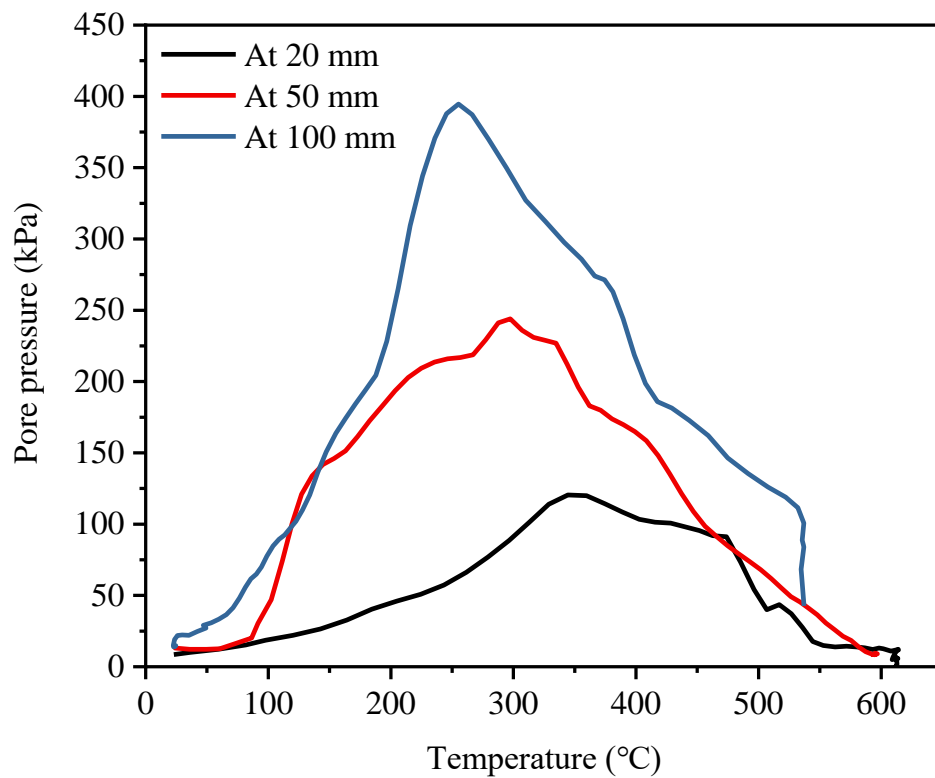
Fig. 12. Pore pressure evolution of specimen RTPF12 at 20, 50 and 100 mm from the heated face.
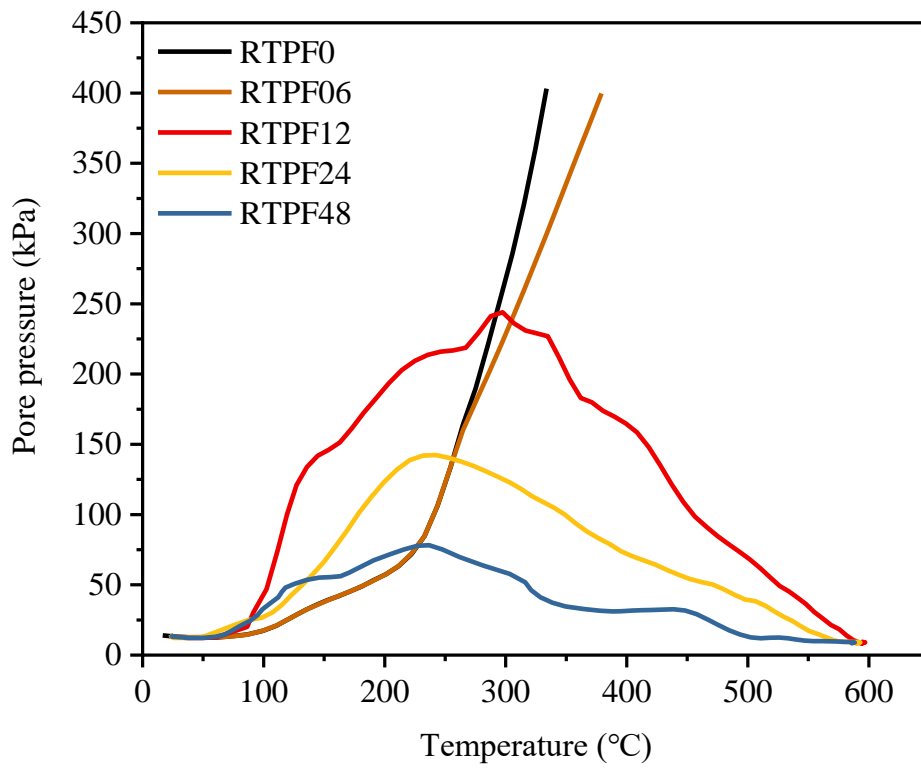
Fig. 13. Pore pressure evolution of concrete with various RTP fibre content at 50 mm.

(a) RTPF0 (20 ℃)　　　　(b) RTPF0 (400 ℃)　　　　　　(c) RTPF0 (600 ℃)

(d) RTPF24 (20 ℃)　　　(e) RTPF24 (400 ℃)　　　　　(f) RTPF24 (600 ℃)
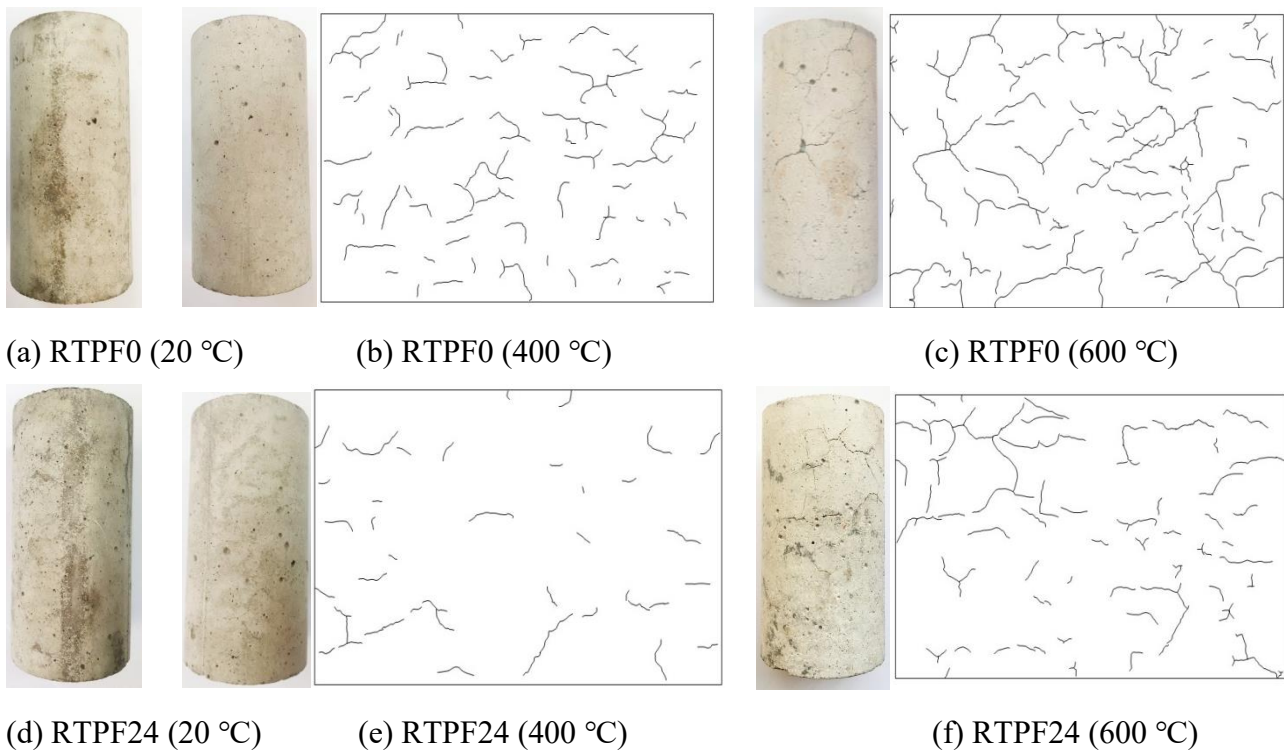
Fig. 14. Surface cracks of specimens RTPF0 and RTPF24 at 20, 400 and 600 ℃.
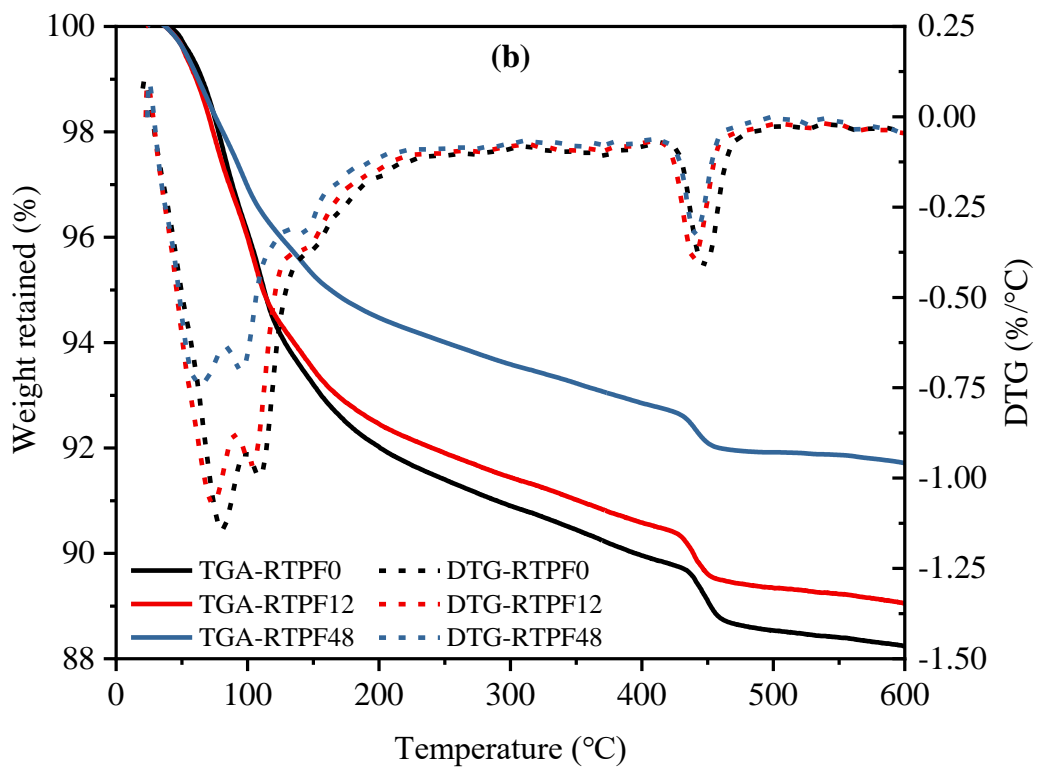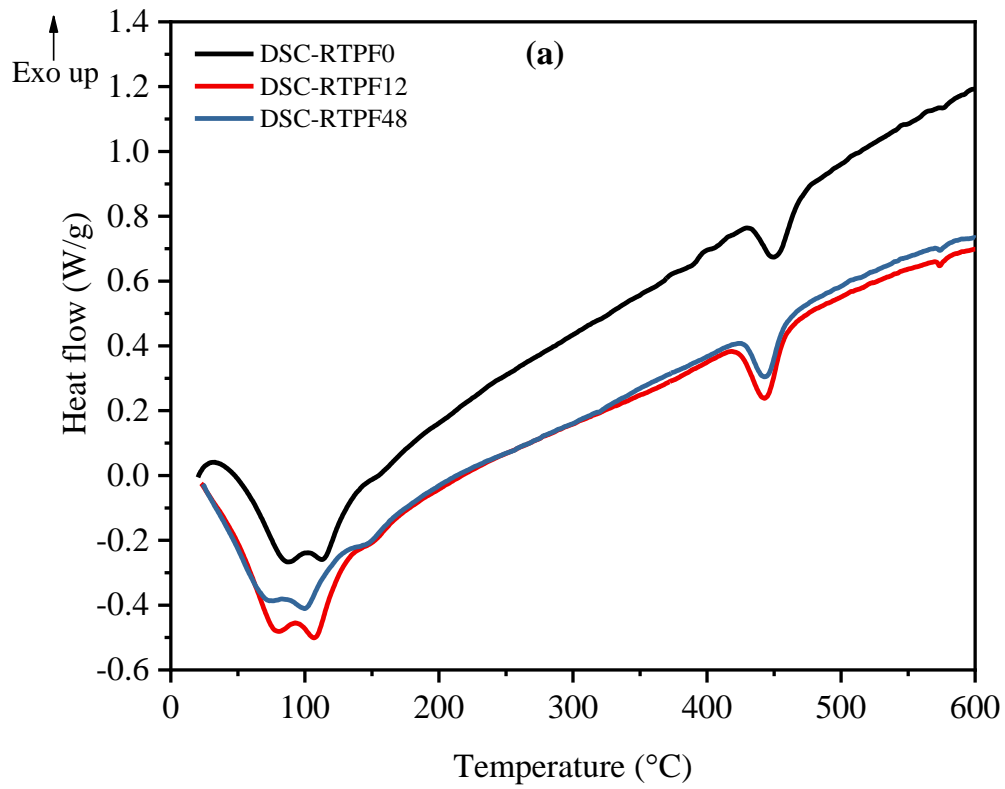
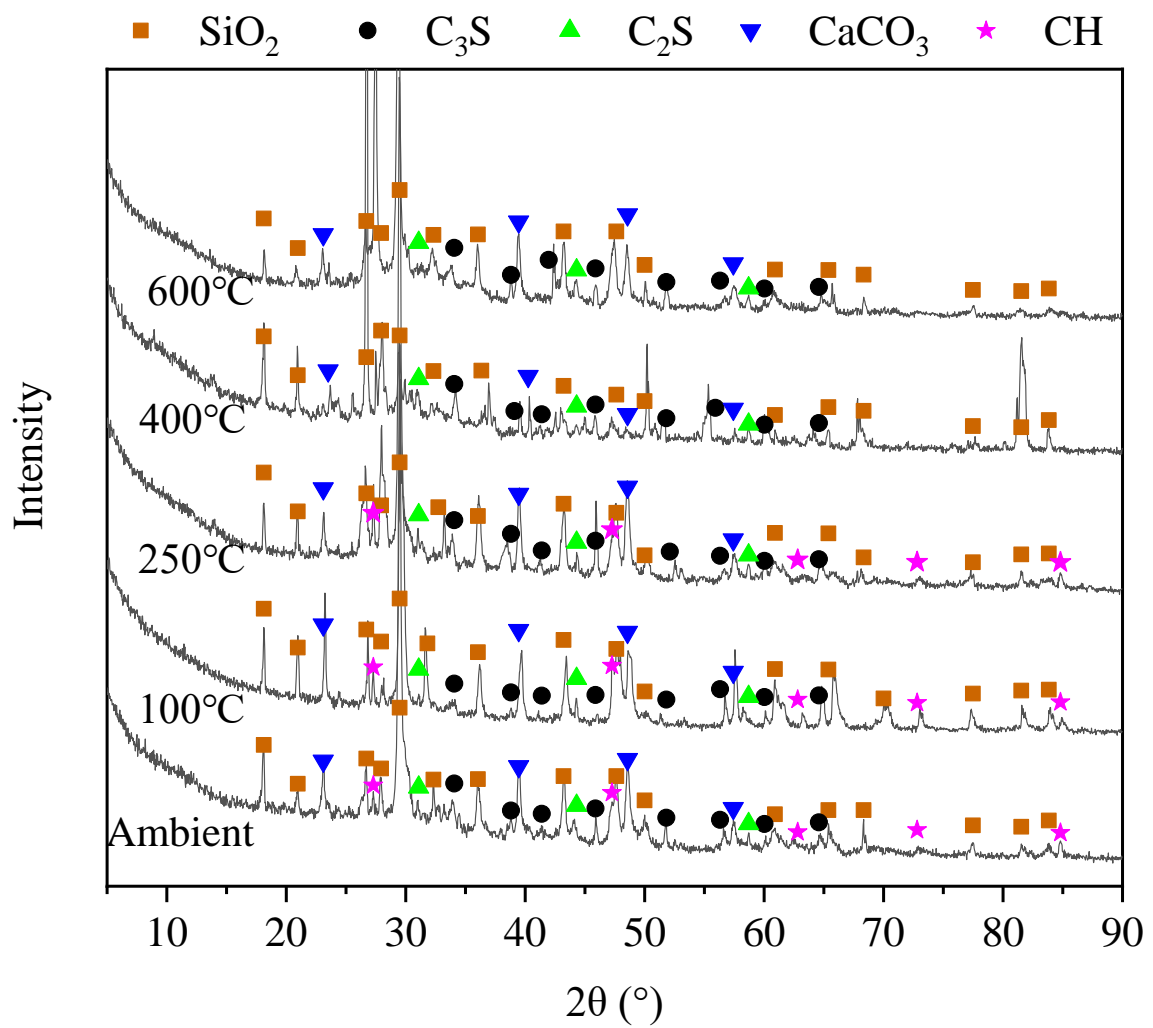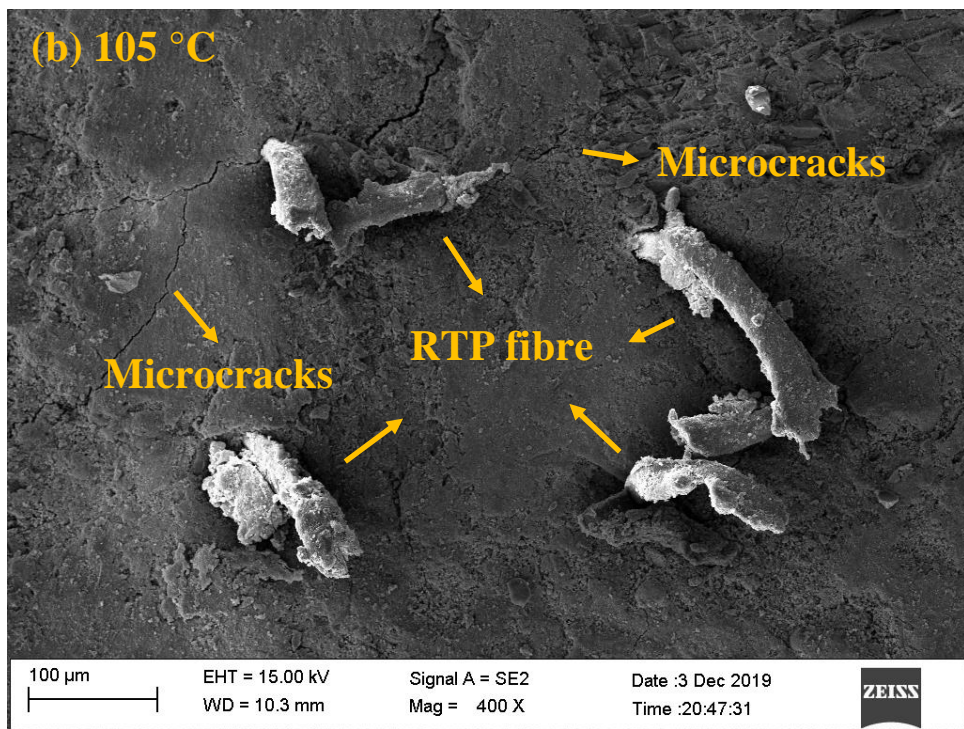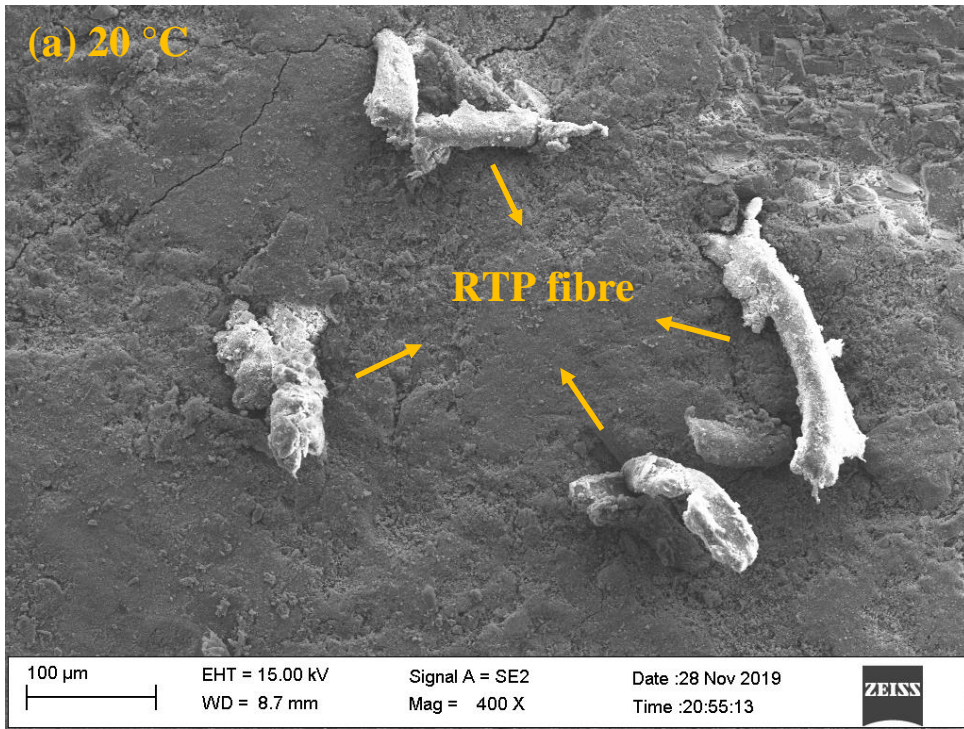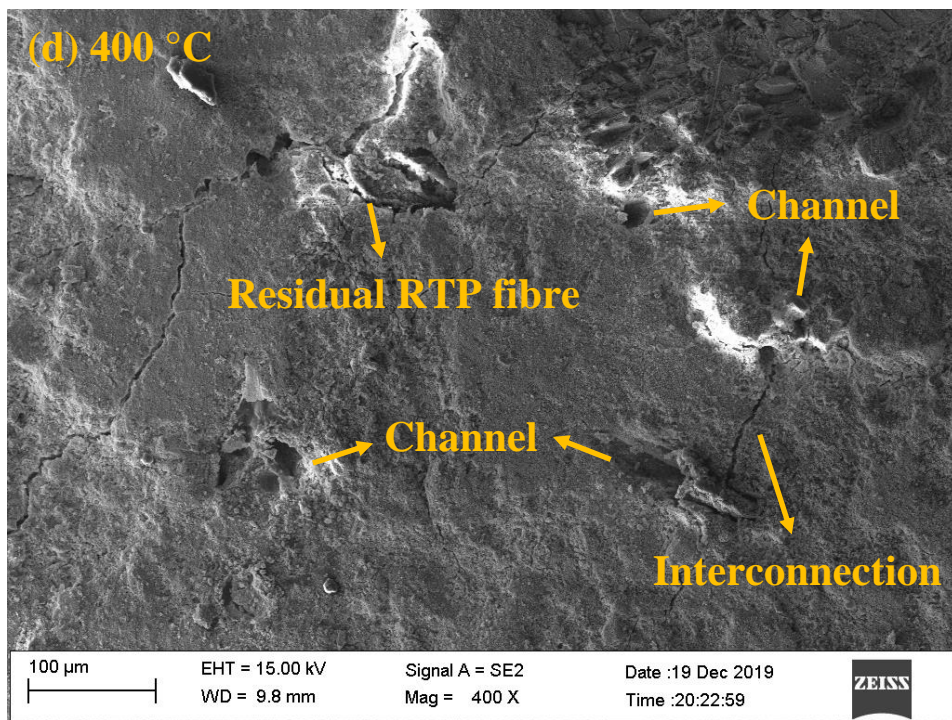Fig. 15. (a) DSC and (b) TGA and DTG curves of concrete with various RTP fibre content.

Fig. 16. XRD spectra of specimen RTPF0 at elevated temperatures.

(a) 20 °C

RTP fibre

100 μm | EHT = 15.00 kV | Signal A = SE2 | Date :28 Nov 2019
WD = 8.7 mm | Mag = 400 X | Time :20:55:13

(b) 105 °C

Microcracks

Microcracks

RTP fibre

100 μm | EHT = 15.00 kV | Signal A = SE2 | Date :3 Dec 2019
WD = 10.3 mm | Mag = 400 X | Time :20:47:31

(c) 250 °C

Residual RTP fibre

New microcracks

| 100 μm | EHT = 15.00 kV | Signal A = SE2 | Date :12 Dec 2019 | ZEISS |
| | WD = 10.4 mm | Mag = 400 X | Time :20:51:43 | |

(d) 400 °C

Residual RTP fibre

Channel

Channel

Interconnection

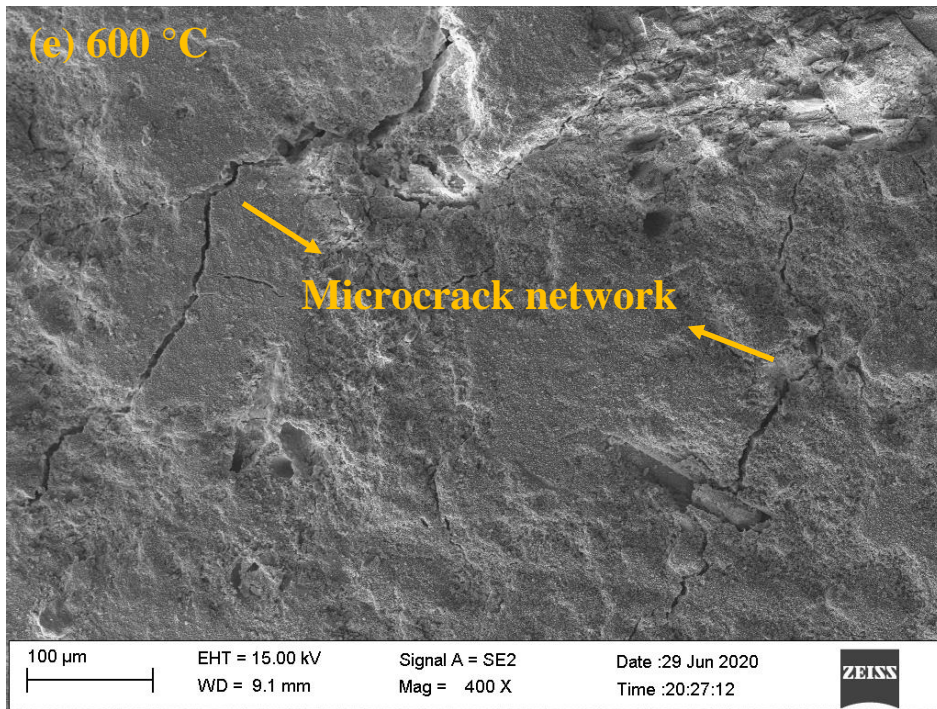| 100 μm | EHT = 15.00 kV | Signal A = SE2 | Date :19 Dec 2019 | ZEISS |
| | WD = 9.8 mm | Mag = 400 X | Time :20:22:59 | |

33

Fig. 17. Microstructural evolution of specimen RTPF48 at (a) 20 °C; (b) 105 °C; (c) 250 °C; (d) 400 °C; (e) 600 °C.
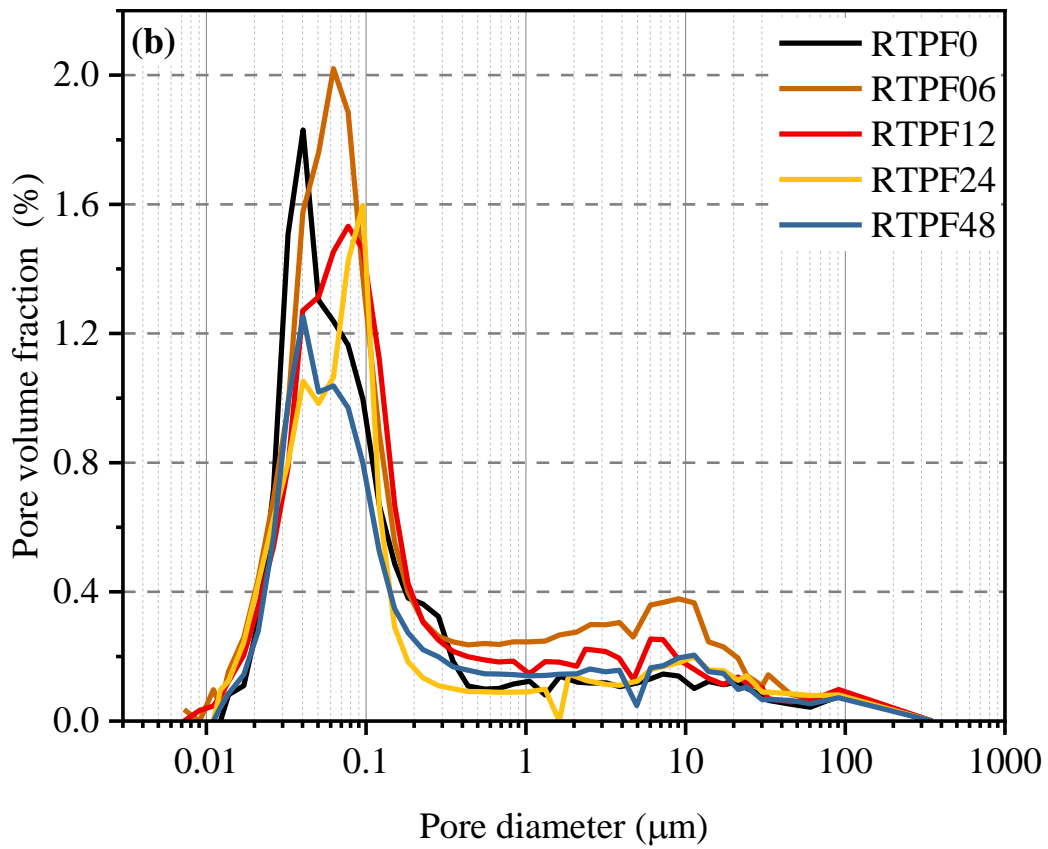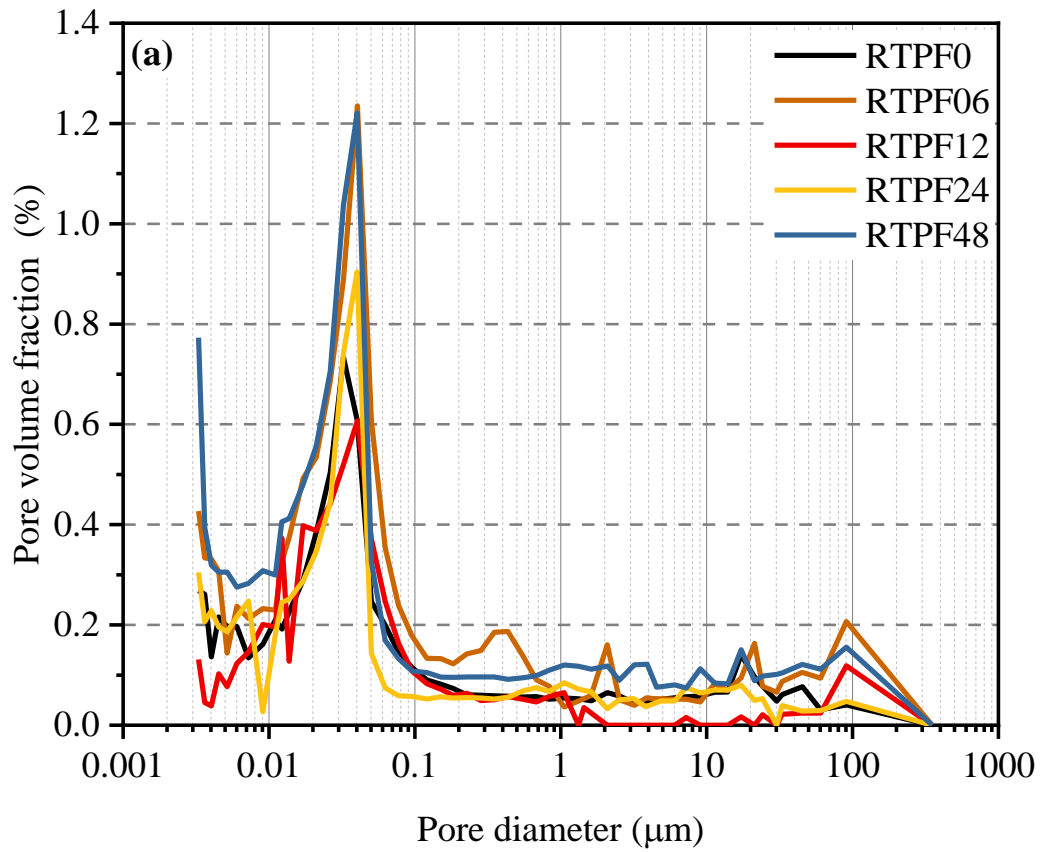
Fig. 18. Pore size distribution of concrete with various RTP fibre content at (a) 20 °C; (b) 600 °C.
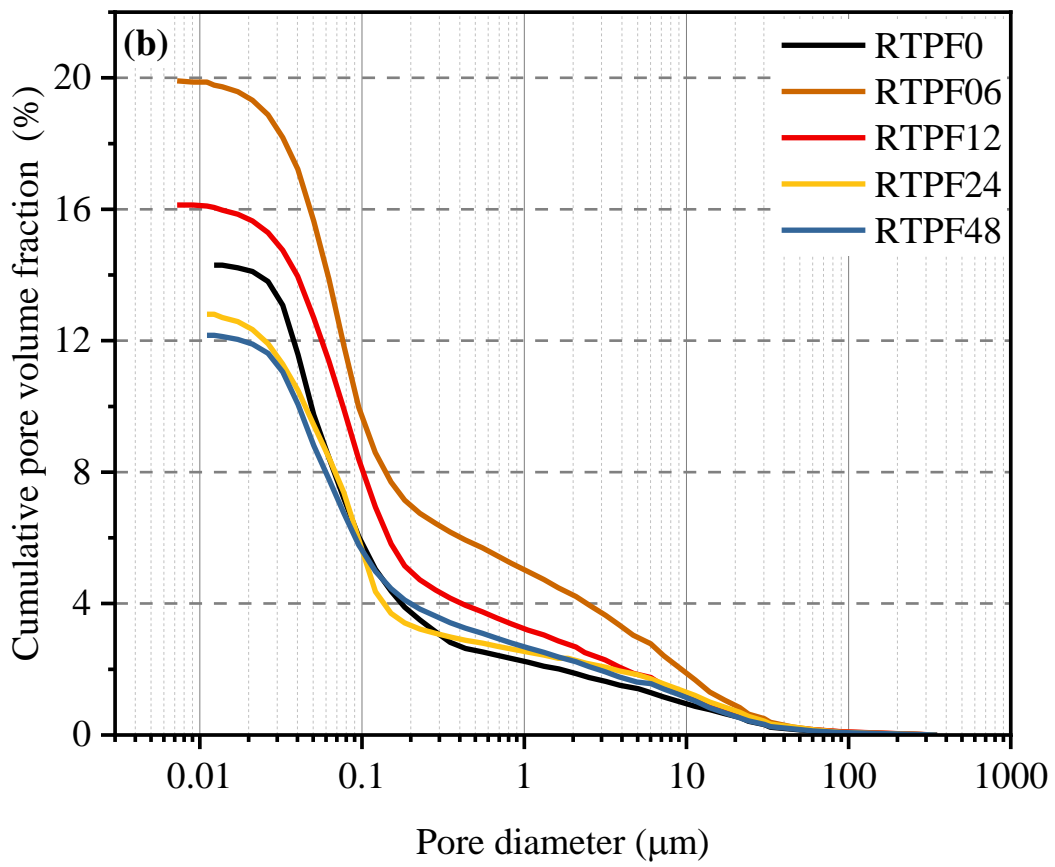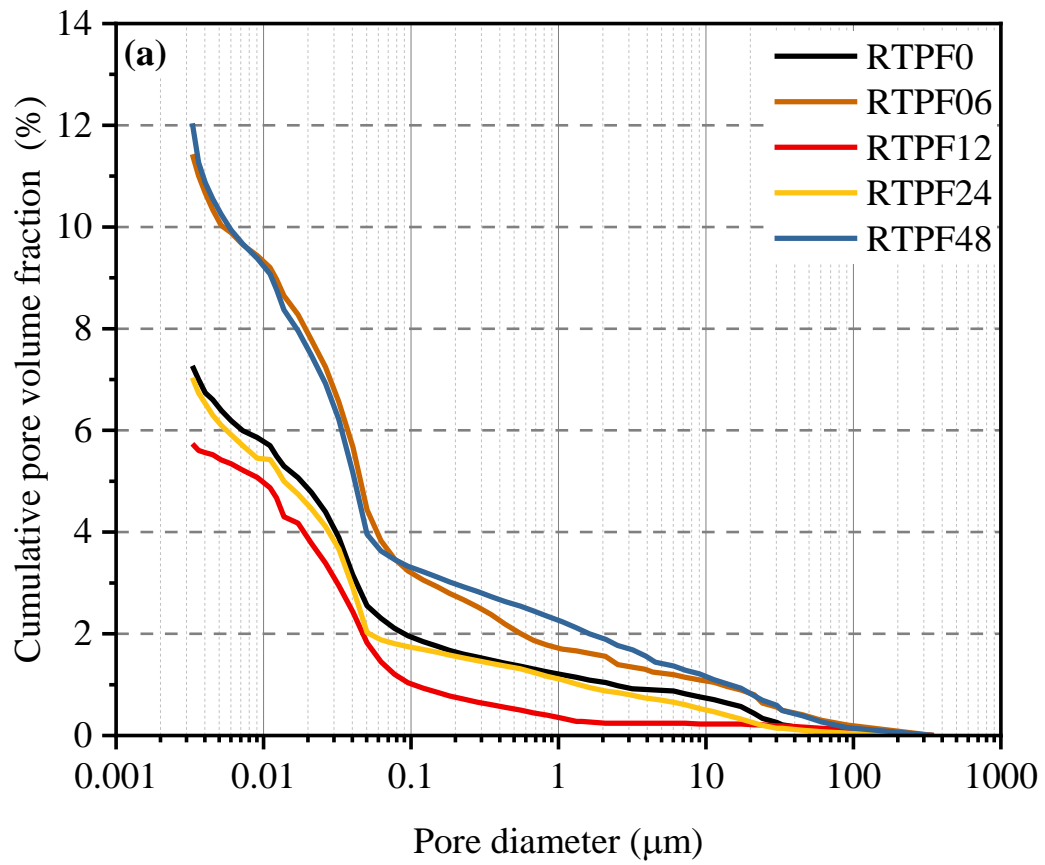
Fig. 19. Cumulative pore volume of concrete with various RTP content at (a) 20 °C; (b) 600 °C.
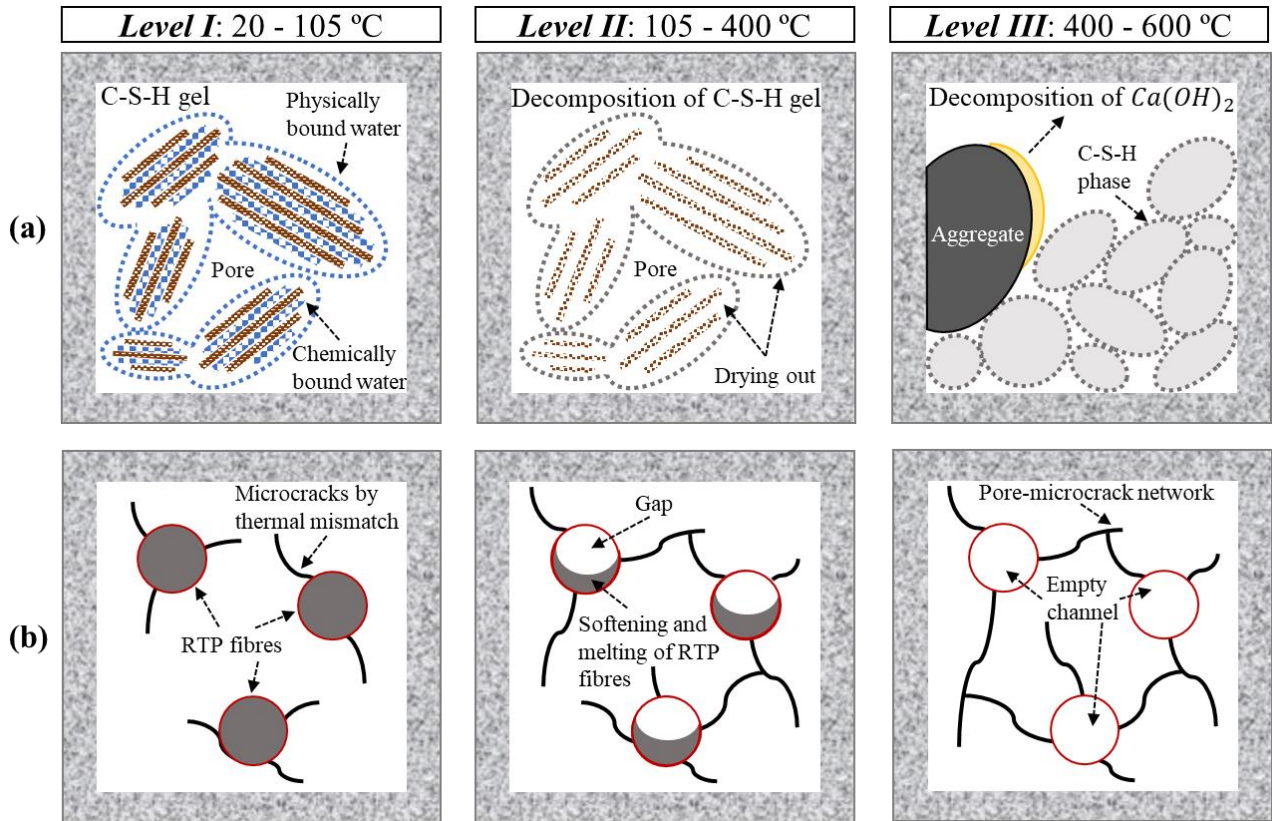
Fig. 20. Schematic demonstration of microstructure of (a) concrete matrix and (b) RTP fibres at elevated temperatures.

Table 1. Chemical composition of cement (wt%).

Oxide	CaO	SiO_2	Al_2O_3	Fe_2O_3	MgO	SO_3	Na_2O	LOI
Cement	60.56	21.35	5.98	2.91	2.22	2.05	0.21	4.72

Table 2. Properties of recycled tyre polymer (RTP) fibre.

Length (mm)	Diameter (µm)	Density (kg/m^3)	Melting point (°C)	Vaporisation point (°C)	Tensile strength (MPa)	Elastic modulus (GPa)
8.7±4.1	21.1±2.5	1160	256	413	475	3.21

Table 3. Mix proportions of RTP fibre reinforced concrete.

Symbol	Cement (kg/m^3)	FA (kg/m^3)	CA (kg/m^3)	Water (kg/m^3)	SP (kg/m^3)	RTP fibre (kg/m^3)	RTP fibre (vol%)
RTPF0	472	616	1144	218	2.36	0.0	/
RTPF06	472	616	1144	218	2.36	0.6	0.05
RTPF12	472	616	1144	218	2.36	1.2	0.1
RTPF24	472	616	1144	218	2.36	2.4	0.2
RTPF48	472	616	1144	218	2.36	4.8	0.4

Note: FA (fine aggregate); CA (coarse aggregate); SP (superplasticiser)